# Design and Evaluation of Nano-Segregated Ionic Liquid/Zwitterion Mixtures

**Zwitterion/**イオン液体混合系のナノレベルの相分離状態の設計とその評価

**Satomi Taguchi**

**2014**

**Department of Biotechnology**
**Tokyo University of Agriculture and Technology**

# Contents

# Chapter 1

## Phase behavior of ionic liquid mixtures

# 1-1 Ionic liquids

## 1-1-1 Definition and characters of ionic liquids

Ionic liquids (ILs) are liquids consisting solely of ions. ILs have received great attention due to their properties, which include negligible vapor pressure, high thermal stability and high ionic conductivity. (Figure 1-1) In general, these properties are quite different from those of molecular solvents.

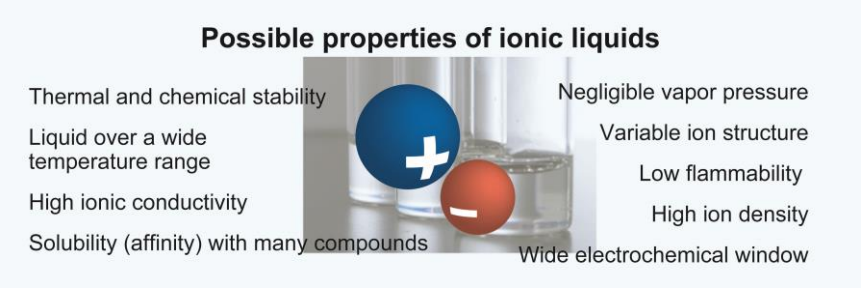


**Figure 1-1** Photograph of ILs and their possible properties.

ILs are not new; some have been known for many years. For instance ethylammonium nitrate[1], which has a melting point of 12 °C, was first described in 1914. $AlCl_4$ salts such as $[C_2mim][AlCl_4]$[2] are reported to be liquid at room temperature. However, these salts are not stable in water. Since the discovery of "air and water" stable imidazolium-type ILs by Willkes in 1992[3], many ILs and their remarkable utility in various fields, including as reaction media[4], electrolyte solutions[5] and bioscience media[6], have been extensively explored. ILs have garnered much attention with 50.000 papers published in this decade.

The commonly used definition that the melting point of ILs is lower than 100 °C[4] is arbitrary and has no physical meaning. However, it has become popular because it represents a condition for materials that these are easier to handle than salts that melt at elevated temperatures.

ILs are designer solvents whose chemical and physical properties can be tuned through the cation and the anion combination. Figure 1-2 shows typical ions used as IL components. ILs contain organic cations, usually quaternized aromatic and aliphatic ammonium. Alkylphosphonium cations have garnered attentions due to their high thermal- and chemical-stability.[7,8] R is commonly an alkyl group, however the properties and functions of the ILs can be controlled by introducing functional groups into R. The IL anions are either inorganic or organic. With the exception of halide anions, the negative charge is usually distributed over several atoms. Fluorinated ions, for example, bis(trifluoromethylsulfonyl)imide ($[Tf_2N]$), tetrafluoroborate ($BF_4$) and hexafluoroborate ($PF_6$), are commonly reported component ions. Recently, non-fluorinated anions, such as carboxylic acids[9] and amino acids[10], have been reported.

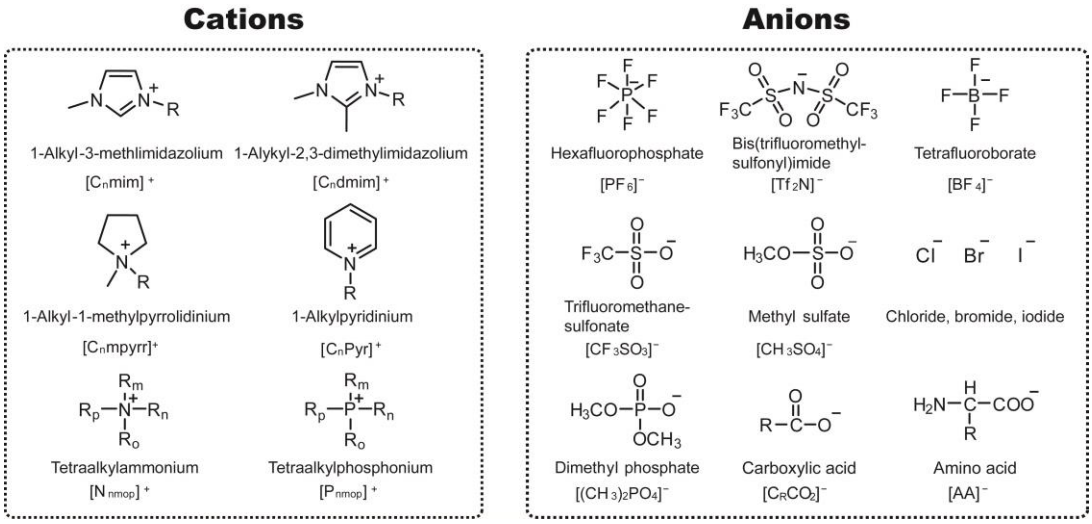


**Figure 1-2** Some common ions used in ILs and their abbreviations.

There are three types of ILs based on their composition, aprotic, protic[11] and zwitterionic[12]. The most heavily researched type is aprotic ILs. Protic ILs are closely related to aprotic ILs except that their cation was formed via the transfer of a proton from a Brønsted acid to a Brønsted base. The cation and anion in a zwitterion are tethered via a covalent bond. More information on this class is given in section 1-1-4.

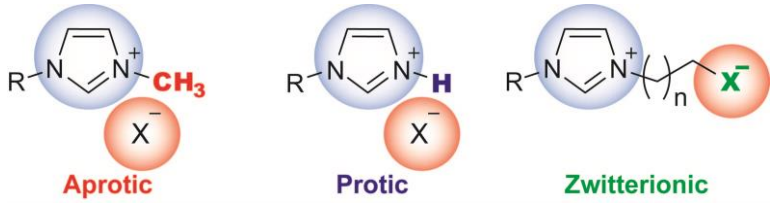


**Figure 1-3** Illustration of each class of ILs, aprotic, protic and zwitterionic.

## 1-1-2 Physico-chemical properties of ionic liquids

### Thermal properties

The characteristic properties of ILs are known to vary based on the choice of the anion and cation. Changes in the size, shape, symmetry and character of the component ions influence the melting points of the salts. The dominant force acting on an IL is the Coulombic attraction between the cation and anion. In addition, the melting point of the ILs is affected by the specific interactions (hydrogen bonds, van der Waals forces and π-π interactions) between the component ions.

- Effect of the anion structure on the ionic liquid melting point

As the anion size increases, the melting point of the salt decreases. Increasing the radius of the anion from the Cl anion to the $PF_6$ anion decreases the melting point of the sodium salts from 801 to 200 ºC. Moreover, anions with a delocalized charge and multiple different conformations have lower melting points. One such ion is the $Tf_2N$ anion, which has extremely electron-withdrawing $CF_3SO_2$- groups conjugated and linked via flexible S-N-S bonds. When combined with the [$C_2$mim] cation, this anion produces a fluid at room temperature. The melting point of this salt is −3 ºC.[9]

- Effect of the cation structure on the ionic liquid melting point

The size and shape of the cation in an IL are important for controlling the melting point of the salt. ILs contain organic cations that are large relative to inorganic cations. These cations significantly reduce the melting point. For instance, the melting points of salts containing the Cl anion decrease from 801 ºC for the Na cation to 87 ºC for the [$C_2$mim] cation. In addition, the melting point of the ILs is related to the cation symmetry.[13] The melting point of an IL composed of a cation with 20 carbon atoms in alkyl chains and the $ClO_4$ anion decreased from 118 ºC for the [$N_{5555}$] cation to 47 ºC for the [$N_{6662}$] cation.[14]

Changes in the melting point of [$C_n$mim][$BF_4$] after making simple changes in a single alkyl-chain substituent are shown in Figure 1-4.[15] Increasing the alkyl chain length ($n < 10$) initially decreased the IL melting point. However, elongation of the alkyl chain further increased the van der Waals forces between the alkyl chains. As a result, the IL melting point increased and liquid crystalline phase was formed. The degree of branching within the alkyl chain also affected the IL melting point. The melting point of an isometric IL increased with an increasing degree of chain branching.

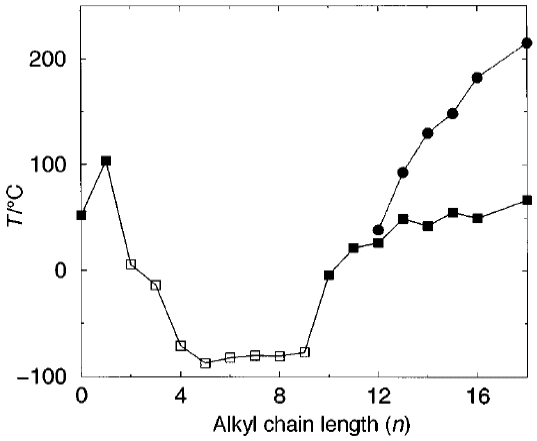


**Figure 1-4** Phase diagram for [$C_n$mim][$BF_4$]. The melting (■), glass (□), and clearing (●) transitions are measured by DSC.

## Viscosity

The IL viscosity is over 100 times larger than that of molecular solvents. For a series of ILs containing the same cation, changing the anion structure clearly affects the viscosity. The viscosity general increases with respect to the anion in order of $Tf_2N$, $CF_3CO_2$ and $BF_4$ (Table 1-1). Obviously, this trend does not exactly correlate to the anion size. The viscosity of an IL is mainly affected by the anion properties, such as their ability to form hydrogen bonds with the cation. In fact, X-ray measurements of [$C_2$mim]Cl show that strong hydrogen bonds exist between the imidazolium cation and the Cl anion.[16] However, the ILs containing the $Tf_2N$ anion, whose charge is delocalized, have lower viscosities.

The IL viscosity is also affected by the identity of the cation. Long alkyl chains within the cation form more viscous fluids. For instance, ILs containing the imidazolium cation and the $Tf_2N$ anion exhibit an increasing viscosity from the [$C_2$mim] cation to the [$C_4$mim] cation to the [$C_8$mim] cation. (Table 1-1)

**Table 1-1** Viscosity data for several ILs at 25 °C.

| IL | Viscosity/cp | ref | IL | Viscosity/cp | ref |
|---|---|---|---|---|---|
| [$C_4$mim]I | 1110 | 17 | [$P_{4441}$][$Tf_2N$] | 207 | 18 |
| [$C_4$mim]$BF_4$ | 219 | 17 | [$P_{4448}$]$BF_4$ | 1240 | 18 |
| [$C_4$mim]$CF_3CO_2$ | 70 | 19 | [$P_{4448}$]$CF_3SO_3$ | 778 | 18 |
| [$C_4$mim]$CF_3SO_3$ | 90 | 9 | [$P_{4448}$]$CF_3CO_2$ | 453 | 18 |
| [$C_4$mim][$Tf_2N$] | 69 | 20 | [$P_{4448}$][$Tf_2N$] | 250 | 18 |
| [$C_6$mim][$Tf_2N$] | 68 | 19 | [$P_{8888}$][$Tf_2N$] | 418 | 21 |
| [$C_8$mim][$Tf_2N$] | 93 | 22 | [$P_{8888}$][Ala] | 1620 | 23 |

## Density

The IL density is higher than 1.0 g/cm$^3$ because ILs consist entirely of ions. Elongating of alkyl chains in the ions decreases the IL density by reducing the Coulombic attraction between the cation and the anion. Molecular solvents, such as alkanes and alcohols, show the opposite tendency because van der Waals dominates them. For instance, the density of an IL composed of substituted imidazolium cation and the $CF_3SO_3$ anion decreased from 1.39 g/cm$^3$ for the [$C_2$mim] cation to 1.29 g/cm$^3$ for the [$C_4$mim] cation. The density of phosphonium cations with long alkyl chains was reported as less than 1.0 g/cm$^3$.[18, 23] For ILs containing the same cation species, increasing the anion mass increases the IL density. Generally, the order of increasing density for ILs composed of a single cation is $BF_4$ anion < $CF_3CO_2$ anion < [$Tf_2N$] anion.

**Table 1-2** Density data for several ILs.

| IL | Density, g/cm$^3$ | Temperature, °C | ref | IL | Density, g/cm$^3$ | Temperature, °C | ref |
|---|---|---|---|---|---|---|---|
| [$C_2$mim]$CF_3SO_3$ | 1.39 | 20 | 9 | [$P_{4441}$][$Tf_2N$] | 1.28 | 25 | 18 |
| [$C_4$mim]$BF_4$ | 1.37 | 25 | 17 | [$P_{4448}$]$BF_4$ | 1.02 | 25 | 18 |
| [$C_4$mim]$CF_3CO_2$ | 1.30 | 25 | 22 | [$P_{4448}$]$CF_3SO_3$ | 1.08 | 25 | 18 |
| [$C_4$mim]$CF_3SO_3$ | 1.29 | 20 | 9 | [$P_{4448}$]$CF_3CO_2$ | 1.03 | 25 | 18 |
| [$C_4$mim][$Tf_2N$] | 1.43 | 25 | 20 | [$P_{4448}$][$Tf_2N$] | 1.18 | 25 | 18 |
| [$C_6$mim][$Tf_2N$] | 1.37 | 25 | 20 | [$P_{8888}$][$Tf_2N$] | 1.07 | 25 | 21 |
| [$C_8$mim][$Tf_2N$] | 1.32 | 25 | 20 | [$P_{8888}$][Ala] | 0.903 | 25 | 23 |

## Polarity

Chemists usually attempt to understand the effects of the solvent on a chemical process in terms of its polarity. The most common polarity measurement used by chemists is the dielectric constant. The value of the dielectric constant of an IL cannot be directly measured because truly direct measurements require a non-conducting medium. Other methods for determining the IL polarity have been used, such as chromatographic measurements[24], solvatochromic dyes[25] and chemical reactions[26]. Solvatochromic dyes are widely used to evaluate the IL polarity.

The UV-vis absorption and fluorescence spectra of a chemical compound are known to be influenced by the surrounding medium, such as the solvent. This phenomenon is termed *solvatochromism*. Solvatochromic dyes were first suggested as visual indicators of the solvent polarity by Brooker *et al.*[27]; however the first spectroscopic solvent polarity scale was developed by Kosower. This scale was called the Z-scale and used the intermolecular charge-transfer absorption of 1-ethyl-4-(methoxycarbonyl)pyridinium iodide as the probe.[28] Since then, various UV-vis based

solvent polarity scales have been developed. Notably, the $E_T(30)$ scale is one of the most widely used empirical polarity scales. The $E_T(30)$ values use negatively solvatochromic Rechardt's dye 30 (Figure 1-5) as the probe molecule and are simply defined as the molar electronic transition energies ($E_T$) of the dissolved dye (eqn 1-1).

$$E_T(30)\ \text{kcal/mol} = hcN_A/\lambda_{max} \quad \text{(eqn 1-1)}$$

1,3-Dialkyl substituted imidazolium ILs give similar values to those obtained for short chain primary alcohols (ethanol = 51.9 kcal/mol[32]), while 1,2,3-trisubstiuted imidazolium ILs have noticeably lower $E_T(30)$ values, which are similar to those of secondary alcohols (Propan-2-ol = 48.4 kcal/mol[32]).

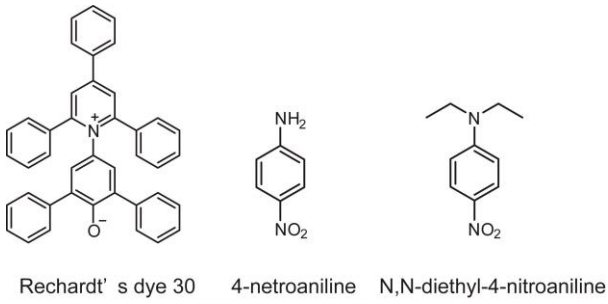


**Figure 1-5** Structure of the dyes.

A more rigorous approach for determining multiple interaction solvent effect has been reported by Kamlet and Taft.[29] This method was called the Kamlet-Taft parameter and used three dyes (Rechardt's dye 30, 4-netroaniline and N,N-diethyl-4-nitroaniline, Figure 1-5). The Kamlet-Taft value details three solvent properties, the hydrogen bond acidity ($\alpha$), hydrogen bond basicity ($\beta$) and dipolarity/polarizability ($\pi^*$). The $\alpha$, $\beta$ and $\pi^*$ values were calculated by use of the following equations.

$$\nu_{(dye)} = 1/(\lambda_{max\ (dye)} \times 10^{-4}) \quad \text{(eqn 1-2)}$$

$$\pi^* = 0.314(27.52 - \nu_{(N,N\text{-diethyl-4-nitroaniline})}) \quad \text{(eqn 1-3)}$$

$$\alpha = 0.0649\ E_T(30) - 2.03 - 0.72\pi^* \quad \text{(eqn 1-4)}$$

$$\beta = (1.035\nu_{(N,N\text{-diethyl-4-nitroaniline})}) + 2.64 - \nu_{(4\text{-nitroaniline})})/2.80 \quad \text{(eqn 1-5)}$$

The $\pi^*$ values for the ILs are high relative to non-aqueous molecular solvents. Although the differences between ILs are small, both the cation and the anion affect the value. The $\beta$ values of the ILs are dominated by anion nature. The $\alpha$ values of the ILs are largely determined by the cation nature, there is also a small anion effect. ILs containing the [$C_4$dmim] cation have low $\alpha$ values, which reflect the loss of a proton in the 2-position of the imidazolium ring.

**Table 1-3** $E_T(30)$ and Kamlet-Taft values for a selection of ILs[30].

| Solvents | $E_T(30)$ Kcal mol$^{-1}$ | Kamlet-Taft values | | |
|---|---|---|---|---|
| | | $\pi^*$ | $\alpha$ | $\beta$ |
| [$C_4$mim][$BF_4$] | 52.5[31] | 1.047 | 0.627 | 0.376 |
| [$C_4$mim][$PF_6$] | 52.3 | 1.032 | 0.634 | 0.207 |
| [$C_4$mim][$CF_3SO_3$] | 52.3 | 1.006 | 0.625 | 0.464 |
| [$C_4$mim][$Tf_2N$] | 51.5 | 0.984 | 0.617 | 0.243 |
| [$C_4$mpy][$Tf_2N$] | | 0.954 | 0.423 | 0.252 |
| [$C_4$dmim][$Tf_2N$] | 48.6 | 1.010 | 0.381 | 0.239 |
| Water | 63.1[32] | 1.33 | 1.12 | 0.14 |
| Methanol | 55.4[32] | 0.60[33] | 0.98[33] | 0.66[33] |
| Acetone | 42.2[32] | 0.704 | 0.202 | 0.539 |
| Dichloromethane | 40.7[32] | 0.791 | 0.042 | −0.014 |

## 1-1-3 Ionic liquid crystals

Liquid crystals combine order and mobility on both the microscopic and macroscopic scale. One example of the functionalization of ILs is the introduction of liquid crystalline (LC) properties to an isotropic IL. Ionic liquid crystals[34] are a class of LC compounds containing anions and cations and can be considered combining the properties of liquid crystals and ILs.

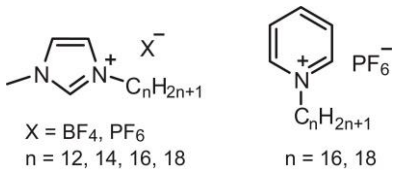


**Figure 1-6** Some ionic liquid crystals having a single long alkyl chain.

Imidazolium-type ILs[35] and pyridinium-type ILs[36] containing long alkyl chains were reported to exhibit LC behaviors (Figure 1-6). The LC phases are induced in these materials by the segregation of the ionic and non-ionic moieties (long alkyl or perfluoroalkyl chain). Most ILs containing a single chain from bilayer smectic structures via the interdigitation of the alkyl chains. The LC properties are also affected by the anion structure. The order of stabilization for the LC structure of 1-alkyl-3-methylimidazolium salts is Cl anion > Br anion > $BF_4$ anion > $PF_6$ anion > $CF_3SO_3$ anion > $Tf_2N$ anion.[37]

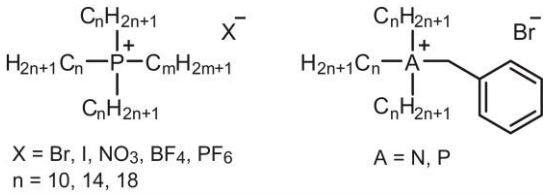


**Figure 1-7** ionic liquid crystals having multiple long alkyl chains.

ILs with multiple long alkyl chains also exhibit LC behavior. For example, Weiss *et al*. reported a series of ammonium and phosphonium salts with three long alkyl chains that exhibit thermotropic smectic phases (Figure 1-7).[38] Thermotropic columnar phases are formed by the self-organization of fan-shaped imidazolium salts (Figure 1-8).[39,40] The analogous ammonium salts form bicontinuous cubic structures (Figure 1-9).[41] ILs with fan-shaped structures have been studied as one-dimensional and three-dimensional ion transport channels.

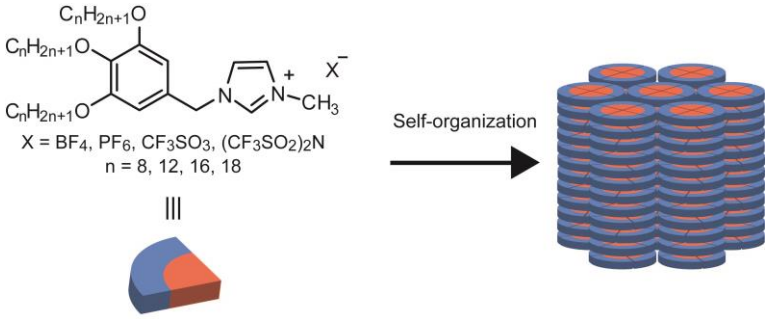


**Figure 1-8** Molecular structure of fan-shaped imidazolium-type salts and schematic illustration of the self-organized structure of them in the hexagonal columnar state.

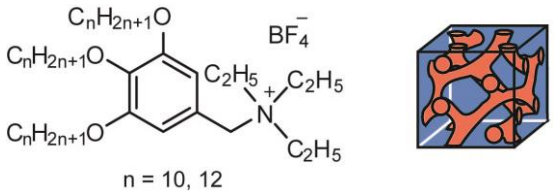


**Figure 1-9** Molecular structure of fan-shaped ammonium-type salts and schematic illustration of the self-organized structure of them in the bicontinuous cubic state.

ILs can self-organize by mixing with amphiphilic or LC molecules.[42] The first report of the amphiphilic self-assembly of an IL to create a LC aggregate was in 1983. Evans *et al*. reported the formation of phospholipid mesophases in ethylammonium nitrate (EAN).[43] More recently, IL and amphiphile systems capable of supporting all of the main lyotropic LC mesophases in EAN, other protic ILs and aprotic ILs, have been reported.[44,45] Protic ILs are similar to water due to their protic nature and general solvent properties, such as polarity, with many of the protic ILs can support self-assembly. Drummond *et al*. reported observing various LC phases in mixtures of protic ILs and hexadecylammonium bromide (CTAB).[44] There have been few investigations into the formation of LC structures in aprotic ILs. A preliminary study was conducted by Tang *et al*. using the non-ionic amphiphile Brij 76 in [$C_4$mim][$BF_4$].[46] Kimizuka *et al*. reported that the combination of ether with aprotic ILs and glycolipids formed a gel and LC state depending on the component concentrations (Figure 1-10).[47] Kato *et al*. reported that the mixture of mesogenic compounds and [$C_2$mim][$BF_4$] formed stable layered LC structures.[48]

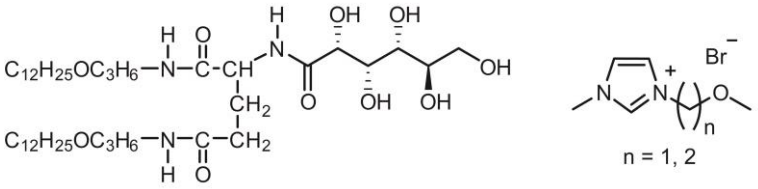


**Figure 1- 10** A combination of glycolipids and ILs forming lyotropic LC systems.

## 1-1-4 Zwitterions

Most electrochemical systems require target carrier ions such as a lithium cation, proton or iodide to construct the corresponding cells. In other words, a matrix that predominantly transports such target ions is required for electrochemical applications. The conductivity of ILs is derived from their component ions, which are mostly useless as target ions. Even when target ions are added to an IL, its component ions still migrate along the potential gradient.

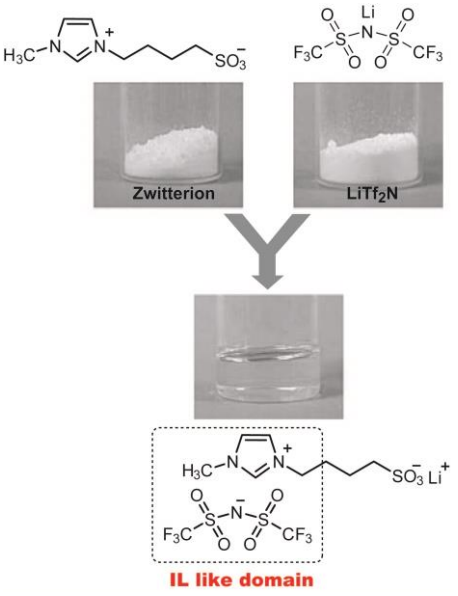


**Figure 1-11** Schematic illustration of zwitterion was mixed with $LiTf_2N$ to form liquid salts.

Some ILs have been designed so that component ions cannot migrate along the potential gradient. One design is the zwitterionic structure, in which the cation is tethered to the anion.[12,49]Based on their structures, zwitterions are not expected to migrate even under a potential gradient. Zwitterions have a high melting temperature ($T_m$). For example the $T_m$ of N-ethylimidazolium methyl sulfonate is 150 °C. This considerable increase in the melting temperature was caused by the decreased mobility of each ion. Despite the high melting point of zwitterions, mixing of a zwitterion with an appropriate salt and acid yielded a liquid at room temperature. For instance, an equimolar mixture of N-ethylimidazolium methyl sulfonate and lithium bis(trifuoromethylsulfonyl)imide (LiTf2N) obtained as liquid. The mixture possessed an ionic conductivity of $7.5\times10^{-6}$ S/cm at 50 °C.[12] This relatively high ionic conductivity and the solid to liquid phase transition were attributed to the IL-like domain formed by the coupling of the zwitterion cation and the added $Tf_2N$ anion. (Figure 1-11) Furthermore, the transference number for lithium cations in this mixture was 0.56.[50] In recent years, zwitterions have been proposed as additives for controlling the IL properties without changing its ion pair.[51,52]

## 1-1-5 Ionic liquid applications

### As battery electrolytes

ILs are interesting as a novel electrolyte system for electrochemical devices such as Li batteries[53,54], capacitors[55], fuel cells[56,57,58] and solar cells[59,60]. ILs attract special attention as the electrolyte for lithium ion batteries because they are non-volatile and flame-resistant nature. The conductivity of ILs containing the [$C_2$mim] cation is approximately 10 mS/cm (14 mS/cm for [$C_2$mim][$BF_4$][61]), similar to lithium salt solutions in cyclic carbonate mixtures. However, pyrrolidinium-type and piperidinium-type ILs have higher electro-suitability than imidazolium-type ILs[62], which exhibit lower conductivities of 1-2 mS/cm (1.9 mS/cm for [$C_4$Pyr][$BF_4$][63]). The target ions must be dissolved in the IL because the IL components are mostly useless as target ions in electrochemical devices. The dissolution of the Li salt in the IL increases the viscosity and decreases the conductivity. [64] The development of IL-based Li ion batteries is still in the preliminary stages, and further progress is needed. However, ILs are still attractive materials because they are thermally and chemically suitable and designable.

### As solvents for reactions

An incredible number of papers have appeared detailing organic reactions and catalyzed processes performed in ILs.[4] The extraction and recycling processes are improved using ILs as the reaction solvent because ILs have designable compatibility with other materials. Seddon *et al*. reported [$C_4$mim][$PF_4$] as a suitable solvent for the Heck reaction.[65] [$C_4$mim][$PF_6$] dissolves the palladium catalyst and allows the products and byproducts to be easily separated using three phase systems (water, cyclohexane and [$C_4$mim][$PF_6$]). Consequently, the catalyst and the IL can be recycled and reused. Davis *et al*. reported that Brønsted acidic ILs containing a sulfonic acid group in the cation are useful solvent and/or catalysts for several organic reactions, including Fischer esterification, alcohol dehydrodimerization and the pinacol rearrangement.[66] Polymerizations were also recently conducted in ILs.[67]

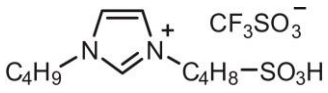


**Figure 1-12** Structures of Brønsted acidic ILs containing a sulfonic acid group.

## As biopolymer solvents

Cellulose is expected to become an alternative to fossil fuels. However, cellulose is rarely used for bioenergy production because of its very poor solubility in common solvents. The chemical and physical stability of cellulose derives from its many intra- and inter-molecular hydrogen bonds. A great deal of energy is needed to break these hydrogen bonds and dissolve cellulose. In 2002, Rogers *et al*. reported that [$C_4$mim]Cl dissolved cellulose above 100 °C due to its polar chloride anion[68,69]. Since then, ILs have been a potential solvent for cellulose. Unfortunately, ILs containing chloride anions have high melting points. Therefore Ohno *et a*l. synthesized imidazolium-type ILs containing phosphorus anions that dissolve cellulose at ambient temperature under mild conditions.[70]

## As solvents for gases

The solubility of various gases in ILs is extremely important for evaluating them as reaction and separation solvents. Researchers have shown large solubility differences between a variety of ILs with relatively high gas solubilities ($CO_2$, $C_2H_4$, $C_2H_6$ and $CH_4$) and low gas solubilities (CO, $H_2$, $O_2$, Ar and $N_2$).[71] Unfortunately, many of the gases used in reactions ($H_2$, $O_2$ and CO) are only sparingly soluble in ILs.

Concern over global climate change has led to an increased interest in $CO_2$ capture technologies. Imidazolium-type ILs containing an amine group to the cation were one of the initial materials studied capturing $CO_2$.[72] The absorption of $CO_2$ by ILs containing amine functionally in the anion has also been reported.[73,74] A high $CO_2$ solubility has been reported for [$C_nC_m$im][$CH_3CO_2$] and is driven by the formation of a zwitterionic 1,3-dialkylimidazolium-2-carboxlate (Figure 1-13).[75] The solubilization of $CO_2$ in ILs occurs through both chemisorption and physisorption. The solubility of $CO_2$ in ILs via physisorption strongly depends on the choice of anion and is highest in ILs with fluoroalkyl anions ([methide] and [$Tf_2N$]) and lowest in ILs with nonfluorinated inorganic anions ([$NO_3$] and [$N(CN)_2$]). The effect of the cation structure on the $CO_2$ solubility is small. Increasing the alkyl chain length from butyl to octyl increased the $CO_2$ solubility.

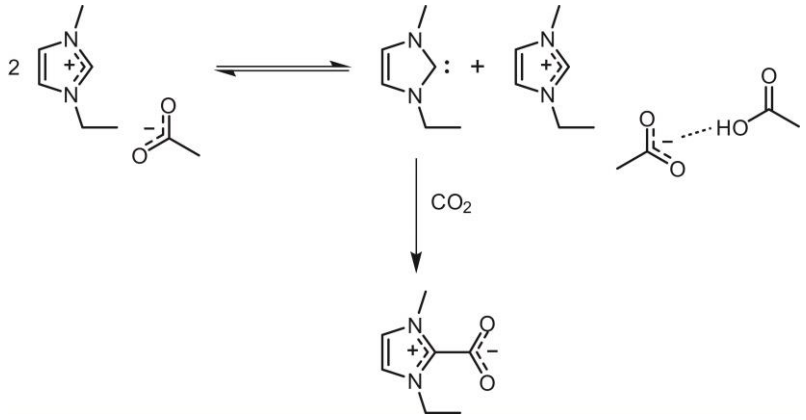


**Figure 1-13** Proposed reaction of $CO_2$ and [$C_2$mim][$CH_3CO_2$].

### 1-1-6 Importance of ionic liquid mixtures

ILs are a class of organic salts in the liquid states at ambient temperature. One of the most attractive features of ILs is their tenability of their functions and properties by designing their cations and anions. A number of ILs have been designed and applied to a wide range of fields.

However, there should be an upper limit to developing ILs with desired functions and properties by only designing their component ions. Recently, increasing attention has been paid to binary or multicomponent IL systems. Many people consider the product of mixing two or more ILs to be a completely new IL. Indeed, on this basis, it has been suggested that $10^{18}$ ILs can be made.[76] IL mixtures are a promising strategy for developing ILs with the desired properties and functions.

## 1-2 Ionic liquid mixtures

Recently, many people have paid particular attention to binary or multicomponent IL systems, because such systems have the potential to function as a new matrix with novel properties that are difficult to obtain using a one-component IL system.[77] When combining two ILs, the obtained IL mixture forms either a monophasic or biphasic system based on the miscibility of each IL. Here, each of these IL mixtures is described.

### 1-2-1 Mixing of miscible ionic liquids

#### Physicochemical properties of ionic liquid mixtures

- Viscosity

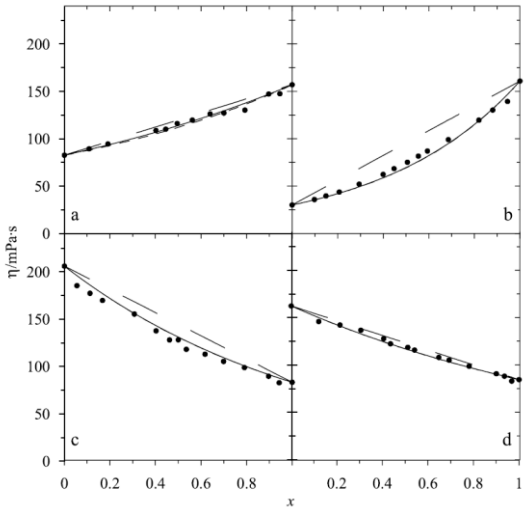


**Figure 1-14** Viscosity against composition for the studied ILs binary systems at T = 303.15 K. Experimental data: (a) $x$[$C_6$mim][$BF_4$] + (1−$x$)[$C_4$mim][$BF_4$]; (b) $x$[$C_6$mim][$BF_4$] + (1−$x$)[$C_2$mim][$BF_4$]; (c) $x$[$C_4$mim][$BF_4$] + (1−$x$)[$C_4$mim][$PF_6$]; (d) $x$[$C_4$mim][$BF_4$] + (1−$x$)[$C_4$mim][$CH_3SO_4$]. Predictions from mixing rules: (– –) $\eta = x\eta_1 + (1- x)\eta_2$; (- - -) Katti and Chaudhri mixing law $\log_{10}(\eta V) = x \log_{10}(\eta_1 V_1) + (1 - x) \log_{10}(\eta_2 V_2) + \Delta g^E/RT$; (—) $\log_{10}(\eta) = x \log_{10}(\eta_1) + (1-x) \log_{10}(\eta_2)$

The viscosities of four series of mixtures, $[C_2mim][BF_4]$+$[C_4mim][BF_4]$, $[C_4mim][BF_4]$+$[C_6mim][BF_4]$, $[C_4mim][BF_4]$+$[C_4mim][PF_6]$ and $[C_4mim][BF_4]$+ $[C_4mim][MeSO_4]$, were measured and compared to four different mixing laws[78] (Figure 1-14). Attempts to fit the data to a simple linear function of the concentration failed, however, two other mixing laws yielded similar and quantitatively accurate results. One is the ideal Katti and Chaudhri mixing law based on the viscosities and molar volumes of the pure components. The other is the Grunberg and Nissen mixing law, which only considers the viscosities.[79] A third mixing law found to agree equally well agreement with the $[C_2mim][BF_4]$+$[C_2mim][N(CN)_2]$ mixture data is that of Bingham, which was developed via an analogy to electric resistors in a parallel circuit.[80]

- Density

Redelo *et al*. analyzed the mixing volumes of $[C_nmim][Tf_2N]$+$[C_mmim][Tf_2N]$, $[C_4mim][PF_6]$+ $[C_4mim][Tf_2N]$, $[C_4mim][BF_4]$+$[C_4mim][Tf_2N]$ and $[C_4mim][BF_4]$+$[C_4mim][PF_6]$ mixtures.[81] The molar volumes of these mixtures changed linearly in accordance with the mole fractions of their components. These results indicate that no new strong chemical interactions form in the mixtures.

However, Navia *et al*. found that mixtures of $[C_4mim][BF_4]$+$[C_4mim][PF_6]$ $[C_4mim][BF_4]$+ $[C_4mim][MeSO_4]$ showed a small negative deviation from the simple linear behavior. They suggested that the availability of free space in ILs containing the $BF_4$ anion could lead to packing effects cause the observed negative deviation. For the $[C_4mim][BF_4]$+$[C_4mim][MeSO_4]$ mixture, the $MeSO_4$ anion being a significantly stronger hydrogen bond accepter than the $BF_4$ anion contributes to this negative deviation.

- Polarity

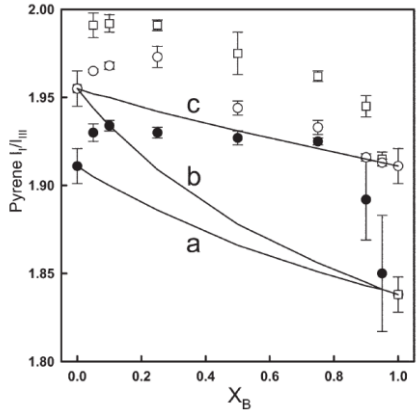


**Figure 1-15** Experimental pyrene $I_I/I_{III}$ values for the binary (A+B) IL systems $[C_4mim][Tf_2N]$+$[C_4mim][PF_6]$ (●), $[C_2mim][Tf_2N]$+$[C_4mim][PF_6]$ (□), and $[C_2mim][Tf_2N]$+ $[C_4mim][Tf_2N]$ (○). $X_B$ denotes the mole fraction for the component "B" in the bulk. Solid lines a–c are the corresponding ideal curves for these mixtures generated from eqn[82].

Solvatochromic probes have been used extensively to evaluate the polarity of not only single-component ILs but also IL mixtures. However, it is important to understand that such probes respond to the solvent species in their immediate environment, the cybotactic region. Therefore, the composition of the cybotactic region does not necessarily reflect the bulk mixture. While it might be expected that the π* value would reflect the spectral changes of pyrene, this was not the case mixtures of [$C_4$mim][$PF_6$], [$C_4$mim][$Tf_2N$] and [$C_2$mim][$Tf_2N$].[83] Despite the π* value of the mixtures changing linearly with the mole fractions of the components, the pyrene spectra in these mixtures deviated strongly from a simple linear behavior. However, the values for simple ILs are very similar, and it would be difficult to detect significant deviations from linear mixing.

The Kamlet-Taft parameters of amino acid IL mixtures have been measured.[84] While the π* values of [$C_2$mim][Ala]+[$C_2$mim][Val] mixtures did not change significantly, both [$C_2$mim][Asp]+[$C_2$mim][Lys] and [$C_2$mim][Glu]+[$C_2$mim][Lys] mixtures deviated strongly towards higher polarities, exceeded the values for the pure components. It seems likely that these results are due to the chemical interactions between the Asp and Glu anions. The α values of the [$C_4$mim][Asp] and [$C_4$mim][Lys] mixtures decreased with increasing [$C_4$mim][Lys].

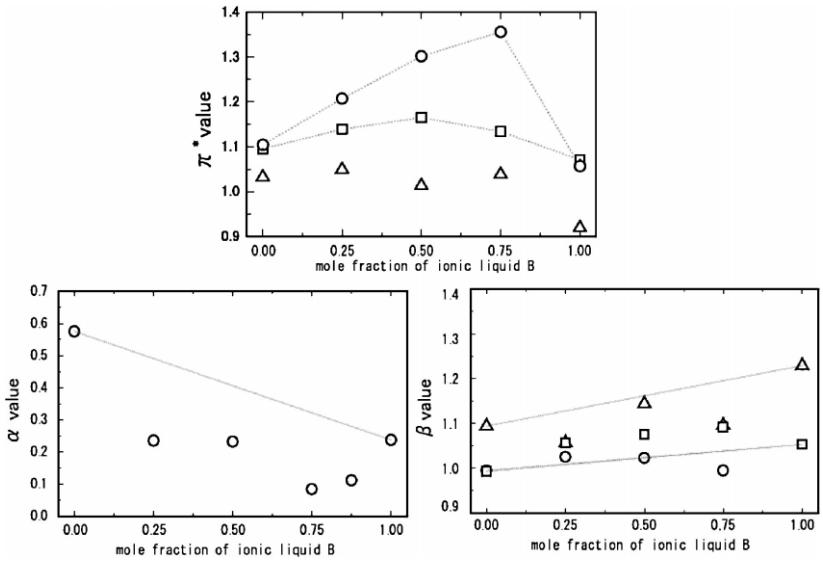


**Figure 1-16** Kamlet–Taft parameters for the amino acid IL mixtures (A + B). [$C_2$mim][Ala] + [$C_2$mim][Val] (△), [$C_2$mim][Asp] + [$C_2$mim][Lys] (○), [$C_2$mim][Glu] + [$C_2$mim][Lys] (□).

- Conductivity

There is no clear description of what would constitute an ideal conductivity for IL mixtures. Only a few examples with significant positive deviation from a simple linear mixing rule have been reported. MacFarlane *et al*. found that the molar conductivity of [$C_2$mim][$Tf_2$N]+ [$C_2$mim][$CF_3SO_3$] mixtures deviated positively from a simple linear mixing rule(Figure 1-17)[85]. Because the self-diffusion constants of the ions did not change significantly with the different compositions, they argued that the decreased ion clustering reduced the correlated ion movement and increased the number of independent charge carriers, which could explain the increased conductivity. Mixtures of [$C_2$mim][$BF_4$]+[$C_2$mim][$N(CN_2)$] also showed a positive deviation from the linear mixing.[86] When 10 wt% of [(NC)$C_1$Cn($C_1$)$_2$N][$Tf_2$N] (n =1 or 2) was added to [$C_2$mim][$Tf_2$N], a sharp increase in the conductivity was seen despite the conductivities of the simple ammonium salts being considerably lower than that of [$C_2$mim][$Tf_2$N].[87] For mixtures of [$C_2$mim][$BF_4$] and [$C_3$mim]Br, the conductivity was found to be less than expected from simple linear mixing.[88] A negative deviation was also found for [$C_4$mim][$BF_4$] and [$C_2$mim][$Tf_2$N] mixtures.[89] This behavior might be indicative of a structural change in the ILs upon mixing and is therefore worthy of further investigation.

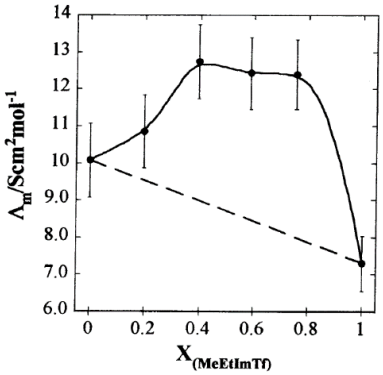


**Figure 1-17** Conductivity of binary composition [$C_2$mim][$Tf_2$N]+ [$C_2$mim][$CF_3SO_3$]. The dashed line in shows the conductivity behavior expected from a simple law of mixtures.

- Ionic liquid mixture applications

ILs have drawn much attention as solvents for chemical syntheses. It is likely that this will hold true for their mixtures. The lipase-catalyzed esterification of glucose with a fatty acid has the highest glucose solubility and initial enzyme activity when using hydrophilic ILs; however, the highest enzyme recyclability was found using hydrophobic ILs. In a combined hydrophobic IL [$C_4$mim][$Tf_2$N] and hydrophilic IL [$C_4$mim][$CF_3SO_3$], the glucose solubility deviated negatively from the linear behavior; however, the initial activity and recyclability of the enzyme deviated positively.[90]

## 1-2-2 Combination of immiscible ionic liquids

Seddon *et al*. reported that the mixture of certain hydrophilic ILs with specific hydrophobic ILs yielded to two distinct phases, particularly when the structures of either the cation or anion were vastly different.[91] $[P_{66614}]Cl$ and $[C_nmim]Cl$ ($n < 6$) form such biphasic systems when mixed. The miscibility of $[P_{66614}][Tf_2N]$ and $[C_2mim][Tf_2N]$ or $[P_{66614}][Tf_2N]$ and $[C_2pyr][Tf_2N]$[92] was found to be temperature dependent. Mixing two different ILs (each consisting of different anions and cations) creates a four-ion mixture, and some of these mixtures are biphasic. It was found that each ion behaves independently when $[C_2mim][CH_3SO_3]$ and $[P_{66614}][Tf_2N]$ or $[C_2mim][CH_3SO_3]$ and $[P_{66614}][PO_2(C_8H_{17})_2]$ are mixed, which form biphasic solutions. They also reported the application of a system ($[P_{66614}][Tf_2N]$+$[C_2mim][Tf_2N]$) to the separation of aromatic and aliphatic hydrocarbons.[93] A metal separation (cobalt and nickel) via solvent extraction using two mutually immiscible ILs system ($[C_2mim]Cl$+$[P_{66614}][PO_2(C_8H_{17})_2]$), was reported by Binnemans *et al*.[94]

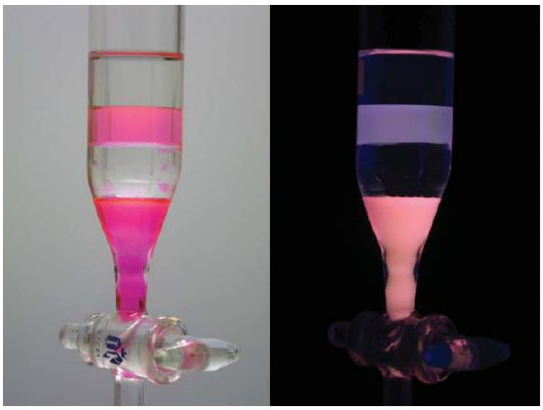

**Figure 1-18** A stable tetraphasic mixture of (from top to bottom): pentane, $[P_{66614}][Tf_2N]$, water and $[C_2mim][Tf_2N]$. The pink coloration is due to rhodamine B dye, which is soluble in the ionic layers. The figure on the left was taken in daylight and the figure on the right was taken under UV illumination (254 nm).

## 1-3 Objectives and outline of this thesis

A simple way to control the chemical and physical properties of ILs is to mix two or more ILs with different properties. Several IL mixtures have been reported. For example, mixing miscible ILs is useful for preparing monophasic IL systems with successively-tuned chemical and thermal properties. Simple mixing does not always give positive results. Mixing of two ILs has a possibility to generate crystalline ion pairs through ion exchange between the ILs. In contrast, combinations of immiscible ILs provide biphasic IL systems, which can be used as separation and reaction media. However, this system does not combine properties and functions of each IL. There is an upper limit to control a phase behavior of IL mixtures by simple mixing of ILs.

The objective of this thesis is to develop a new class of binary IL system where two incompatible ILs coexist homogeneously in a macroscopic scale with keeping their own original properties and functions. The author envisions that these systems will offer a unique opportunity for expanding the potential applications of ILs.

Chapter 1 introduces ILs and describes IL mixtures. The objective of this thesis is also mentioned.

Chapter 2 describes that the zwitterionization of ILs is an effective strategy to improve the miscibility hydrophobic ILs and hydrophilic ILs. The ion pair state in these mixtures is discussed.

Chapter 3 describes the construction of nano-segregated IL systems composed of a phosphonium-type IL with a hydrophilic group and a hydrophilic ammonium-type IL. The relationship between the ion structures and nano-segregated states provides a significant insight into the design of nano-segregated IL systems.

Chapter 4 describes the evaluation of polarity in the nano-segregated IL systems by exploring solvatochromic dyes that dissolve selectively either in hydrophilic or hydrophobic ILs. In addition, the nano-viscosity measurement for the nano-segregated system is mentioned.

Chapter 5 presents the conclusion of this thesis and a discussion of potential future work.

## 1-4 References


1. P. Walden, *Bull. Acad. Imper. Sci*. (St. Petersburg), 1914, 1800.
2. (*a*) F. H. Hurley and T. P. Wier, Jr., *J. Electrochem. Soc.*, 1951, **98**, 203; (*b*) R. J. Gale, B. Gilbert and R. A. Osteryoung, *Inorg. Chem.*, 1978, **17**, 2728; (*c*) J. Robinson and R. A. Osteryoung, *J. Am. Chem. Soc.*, 1979, **101**, 2728.
3. J. S. Willkes and M. J. Zaworotko, *J. Chem. Soc., Chem. Commun.*, 1992, 965.
4. (*a*) P. Wasserscheid and T. Welton, *Ionic Liquids in Synthesis*, Wiley-VCH, Weinheim, 2nd edn, 2008; (*b*) T. Welton, *Chem. Rev.*, 1999, **99**, 2071; (*c*) P. Wasserscheid and W. Keim, *Angew. Chem., Int. Ed.*, 2000, **39**, 3772.
5. (*a*) H. Ohno, *Electrochemical Aspects of Ionic Liquids*, Wiley, 2nd edn, 2011; (*b*) M. Armand, F. Endres, D. R. MacFarlane, H. Ohno and B. Scrosati, *Nat. Mater*., 2009, **8**, 621; (*c*) F. Endres, *ChemPhysChem*, 2002, **3**, 144.
6. (*a*) F. V. Rantwijk and R. A. Sheldon, *Chem. Rev.*, 2007, **107**, 2757; (*b*) U. Kragl, M. Eckstein and N. Kaftzik, *Curr. Opin. Biotechnol.*, 2002, **13**, 565; (*c*) K. Fujita, K. Murata, M. Masuda, N. Nakamura and H. Ohno, *RSC Adv.*, 2012, **2**, 4018.
7. K. J. Fraser and D. R. MacFarlane, *Aust. J. Chem.*, 2009, **62**, 309.
8. J. Kagimoto, K. Fukumoto and H. Ohno, *Chem. Commun.*, 2006, 2254.
9. P. Bonhôte, A-P. Dias, N. Papageorgiou, K. Kalyanasundaram and M. Gra1tzel, *Inorg. Chem.*, 1996, **35**, 1168.
10. K. Fukumoto, M. Yoshizawa and H. Ohno, *J. Am. Chme. Soc.*, 2005, **127**, 2398.
11. (*a*) M. Hirao, H. Sugimoto and H. Ohno, *J. Electrochem. Soc.*, 2000, **147**, 4168; (*b*) H. Ohno and M. Yoshizawa, *Solid State Ionics*, 2002, **154–155**, 303.
12. M. Yoshizawa, M. Hirao, K. Ito-Akita and H. Ohno, *J. Mater. Chem.*, 2001, **11**, 1057.
13. J. Sun, D. R. MacFarlane and M. Forsyth, *Ionics*, 1997, **3**, 356.
14. (*a*) J. E. Gordon and G. N. SubbaRao, *J. Am. Chem. Soc.*, 1978, **100**, 7445; (*b*) J. E. Gordon, *J. Am. Chem. Soc.* 1965, **87**, 4347.
15. J. D. Holbrey and K. R. Seddon, *J. Chem. Soc., Dalton Trans*., **199**, 2133.
16. C.J. Dymek Jr., D. A. Grossie, A. V. Fratini and W. W. Adams, *J. Mol. Struct.*, 1989, **213**, 25.
17. J. G. Huddleston, A. E. Visser, W. M. Reichert, H. D. Willauer, G. A. Broker and R. D. Rogers, *Green Chem.*, 2001, **3**, 156.
18. K. Tsunashima and M. Sugiya, *Electrochemistry*, 2007, **9**, 734.
19. J. M. Crosthwate, M. J. Muldoon, J. K. Dixon, J. L. Anderson and J. F. Brennecke, *J. Chem. Thermodynamics*, 2005, **37**, 559.
20. S. Dzyuba and R. Bartsch, *ChemPhysChem*, 2002, **3**, 161.

21. R. E. D. Sestro, C. Corley, A. Rebertson and J. S. Wilkes, *J. Organomet. Chem.*, 2005, **690**, 2536.
22. S. H. Lee and S. B. Lee, *Chem. Commun.*, 2005, **27**, 3469.
23. J. Kagimoto, S. Taguchi, K. Fukumoto and H. Ohno, *J. Mol. Liq.*, 2010, **153**, 133.
24. J. L. Anderson, J. Ding, T. Welton and D. W. Armstrong, *J. Am. Chem. Soc.*, 2002, **124**, 14247.
25. C. Reichardt, *Green Chem.*, 2005, **7**, 339.
26. S. V. Dzyuba and R. A. Bartsch, *Tetrahedron Lett.*, 2002, **43**, 4657.
27. L. G. S. Brooker, G. H. keyes and D. W. Heseltine, *J. Am. Chem. Soc*. 1951, **73**, 5350.
28. (*a*) E. M. Kosower, *J. Am. Chem. Soc.* 1958, **80**, 3253, 3261, 3267; (*b*) E. M. Kosower, J. A. Skorcz, W. M. Schwarz and J. M. Patton, *J. Am. Chem. Soc.* 1960, **82**, 2188.
29. (*a*) M. J. Kamlet and R. W. Taft, *J. Am. Chem. Soc.*, 1976, **98**, 377; (*b*) R. W. Taft and M. J. Kamlet, *J. Am. Chem. Soc*., 1976, **98**, 2886; (*c*) T. Yokoyama, R. W. Taft and M. J. Kamlet, *J. Am. Chem. Soc.*, 1976, **98**, 3233; (*d*) M. J. Kamlet, J. L. Addoud and R. W. Taft, *J. Am. Chem. Soc.*, 1977, **99**, 6027.
30. L. Crowhurst, P. R. Mawdsley, J. M. Perez-Arlandis, P. A. Salter and T. Welton, *Phys. Chem. Chem. Phys.*, 2003, **5**, 2790.
31. M. J. Muldoon, C. M. Gordon and I. R. Dunkin, *J. Chem. Soc., Perkin Trans. 2*, 2001, **1**, 433.
32. C. Reichardt, *Chem. Rev.*, 1994, **94**, 2319.
33. C. Reichardt, *Solvents and Solvent Effects in Organic Chemistry*, Wiley-VCH, Weinheim, 3rd edn, 2003.
34. K. Binnemans, *Chem. Rev.*, 2005, **105**, 4148.
35. C. J. Bowlas, D. W. Bruce and K. R. Seddon, *Chem. Commun.*, 1996, 1625.
36. C. M. Gordon, J. D. Holbrey, A. R. Kennedya and K. R. Seddon, *J. Mater. Chem.*, 1998, **8**, 2627.
37. A. E. Bradley, C. Hardacre, J. D. Holbrey, S. Johnston, S. E. J. McMath and M. Nieuwenhuyzen, *Chem. Mater.*, 2002, **14**, 629.
38. (*a*) D. J. Abdallah, A. Robertson, H-F Hsu and R. G. Weiss, *J. Am. Chem. Soc.*, 2000, **122**, 3053; (*b*) L. Lu, N. Sharma, G. A. Nagana Gowda, C. L. Khetrapal and R. G. Weiss, *Liq. Cryst.*, 1997, **22**, 23.
39. M. Yoshio, T. Mukai, H. Ohno and T. Kato, *J. Am. Chem. Soc.*, 2004, **126**, 994.
40. M. Yoshio, T. Ichikawa, H. Shimura, T. Kagata, H. Hamasaki, T. Mukai. H. Ohno and T. Kato, *Bull. Chem. Soc. Jpn.*, 2007, **80**, 1836.
41. T. Ichikawa, M. Yoshio, A. Hamasaki, T. Mukai, H. Ohno and T. Kato, *J. Am. Chem. Soc.*, 2007, **129**, 10662.
42. T. L. Greaves and C. J. Drummond, *Chem. Soc. Rev.*, 2008, **37**, 1709.
43. D. F. Evans, E. W. Kaler and W. J. Benton, *J. Phys. Chem.*,1983, **87**, 533.

44. T. L. Greaves, A. Weerawardena, C. Fong and C. J. Drummond, *Langmuir*, 2007, **23**, 402.
45. (*a*) X. Mulet, D. F. Kennedy, T. L. Greaves, L. J. Waddington, A. Hawley, N. Kirby and C. J. Drummond, *J. Phys. Chem. Lett.* 2010, **1**, 2651; (*b*) J. Wang, T. L. Greaves, D. F. Kennedy, A. Weerawardena, G. Song and C. J. Drummond, *Aust. J. Chem.* 2011, **64**, 180.
46. J. Tang, D. Li, C. Sun, L. Zheng and J. Li, *Colloids Surf. A*, 2006, **273**, 24.
47. N. Kimizuka and T. Nakashima, *Langmuir*, 2001, **17**, 6759.
48. M. Yoshio, T. Mukai, K. Kanie, M. Yoshizawa, H. Ohno and T. Kato, *Adv. Mater.*, 2002, **14**, 351.
49. (*a*) M. Yoshizawa, A. Narita and H. Ohno, *Aust. J. Chem.*, 2004, **57**, 139; (*b*) A. Narita, W. Shibayama and H. Ohno, *J. Mater. Chem.*, 2006, **16**, 1475; (*c*) H. Lee, D. B. Kim, S.-H. Kim, H. S. Kim, S. J. Kim, D. K. Choi, Y. S. Kang and J. Won, *Angew. Chem., Int. Ed.*, 2004, **43**, 3053.
50. H. Ohno, M. Yoshizawa and W. Ogihara, *Electrochim. Acta*, 2003, **48**, 2079.
51. Y. Ito, Y. Kohno, N. Nakamura and H. Ohno, *Chem. Commun.*, 2012, **48**, 11220.
52. Y. Ito, Y. Kohno, N. Nakamura and H. Ohno, *Int. J. Mol. Sci.*, 2013, **14**, 18350.
53. (*a*) H. Sakaebe and H. Matsumoto, *Electrochem. Commun.*, 2003, **5**, 594; (*b*) H. Sakaebe, H. Matsumoto and K. Tatsumi, *J. Power Sources*, 2005, **146**, 693; (*c*) H. Matsumoto, H. Sakaebe and K. Tatsumi, *J. Power Sources*, 2005, **146**, 45; (*d*) H. Sakaebe, H. Matsumoto, K. Tatsumi, *Electrochim. Acta*, 2007, **53**, 1048; (*e*) S. Tobishima, *Electrochem.*, 2002, **70**, 198.
54. (*a*) P. C. Howlett, D. R. MacFarlane and A. F. Hollenkamp, *Electrochem. Solid-State Lett.*, 2004, **7**, A97; (*b*) P. C. Howlett, N. Brack, A. F. Hollenkamp, D. R. MacFarlane and M. J. Forsyth, *Electrochem. Soc.*, 2006, **153**, A595.
55. A. B. McEwen, H. L. Ngo, K. LeCompte and J. L. Goldman, *J. Electrochem. Soc.*, 1999, **146**, 1687.
56. M. Doyle, S. K. Choi and G. Proulx, *J. Electrochem. Soc.*, 2000, **147**, 34.
57. M. A. B. H. Susan, A. Noda, S. Mitsushima and M. Watanabe., *Chem. Commun.*, 2003, 938.
58. (*a*) E. Cho, J.-S. Park, S. S. Sekhon, G.-G. Park, T.-H. Yang, W.-Y. Lee, C.-S. Kim and S.-B. Park, *J. Electrochem. Soc.*, 2009, **156**, B197; (*b*) S. S. Sekhon, J.-S. Park, E. Cho, Y-G. Yoon, C.-S. Kim and W.-Y. Lee, *Macromolecules*, 2009, **42**, 2054. (c) S. S. Sekhon, J.-S. Park, J.-S. Baek, S.-D. Yim, T.-H. Yang and C. S. Kim, *Chem. Mater.*, 2010, **22**, 803.
59. (*a*) H. Matsumoto, T. Matsuda, T. Tsuda, R. Hagiwara, Y. Ito and Y. Miyazaki, *Chem. Lett.*, 2001, 26; (*b*) N. Papageorgiou, Y. Athanassov, M. Armand, P. Bonhôte, H. Pettersson, A. Azam and M. Grätzel, *J. Electrochem. Soc.*, 1996, **143**, 3099.
60. (*a*) R. Kawano and M. Watanabe, *Chem. Commun.*, 2003, 330; (*b*) R. Kawano, H. Matsui, C. Matsuyama, A. Sato, M. A. B. H. Susan, N. Tanabe and M. Watanabe, *J. Photochem. Photobiol. A*, 2004, **164**, 87; (c) R. Kawano and M. Watanabe, *Chem. Commun.*, 2005, 2107.
61. J. Fuller, R. T. Carlin and R. A. Osteryoung, *J. Electrochm. Soc.*, 1997, **144**, 3881.

62. H. Sakaebe and H. Matsumoto, *Electrochem. Commun.*, 2003, **5**, 594.
63. A. Noda, K. Hayamizu and M. Watanabe, *J. Phys. Chem. B*, 2001, **105**, 4603.
64. B. Garcia, S. Lavallée, G. Perron, C. Michot and M. Armand, *Electrochimica Acta*, 2004, **49**, 4583.
65. A. J. Carmichael, M. J. Earle, J. D. Holbrey, P. B. McCormac and K. R. Seddon, *Org. Lett.*, 1999, **1**, 997.
66. A. C. Cole, J. L. Jensen, I. Ntai, K. L. T. Tran, K. J. Weaver, D. C. Forbes and J. H. Davis, Jr., *J. Am. Chem. Soc.*, 2002, **124**, 5962.
67. P. Kubisa, *Prog. Polym. Sci.*, 2004, **29**, 3.
68. R. P. Swatloski, S. K. Spear, J. D. Holbrey and R. D. Rogers, *J. Am. Chem. Soc.*, 2002, **124**, 4974.
69. R. C. Remsing, R. P. Swatloski, R. D. Rogers and G. Moyna, *Chem. Commun.*, 2006, 1271.
70. Y. Fukaya, K. Hayashi, M. Wada and H. Ohno, *Green Chem.*, 2008, **10**, 44.
71. J. L. Anthony, J. L. Anderson, E. J. Maginn and J. F. Brennecke, *J. Phys. Chem. B*, 2005, **109**, 6366.
72. E. D. Bates, R. D. Mayton, I. Ntai and J. H. Davis, Jr., *J. Am. Chem. Soc.*, 2002, **124**, 926.
73. B. E. Gurkan, J. C. de la Fuente, E. M. Mindrup, L. E. Ficke, B. F. Goodrich, E. A. Price, W. F. Schneider and J. F. Brennecke, *J. Am. Chem. Soc.*, 2010, **132**, 2116.
74. H. Yu, Y.-T. Wu, Y.-Y. Jiang, Z. Zhoua and Z.-B. Zhang, *New J. Chem.*, 2009, **33**, 2385.
75. G. Gurau, H. Rodríguez, S. P. Kelley, P. Janiczek, R. S. Kalb and R. D. Rogers, *Angew. Chem. Int. Ed.*, 2011, **50**, 12024.
76. J. D. Holbrey and K. R. Seddon, *Clean Technol. Environ. Policy*, 1999, **1**, 223.
77. H. Niedermeyer, J. P. Hallett, I. J. Villar-Garcia, P. A. Hunt and Tom Welton, *Chem. Soc. Rev.*, 2012, **41**, 7780.
78. P. Navia, J. Troncoso and L. Romaní, *J Solution Chem.*, 2008, **37**, 677.
79. L. Grunberg and A. H. Nissan, *Nature*, 1949, **164**, 799.
80. (*a*) A. Stoppa, R. Buchner and G. Hefter, *J. Mol. Liq.*, 2010, **153**, 46; (*b*) E. C. Bingham, *Fluidity and plasticity*, McGraw-Hill, New York, 1922.
81. J. N. C. Lopes, T. C. Cordeiro, J. M. S. S. Esperancüa, H. J. R. Guedes, S. Huq, L. P. N. Rebelo and K. R. Seddon, *J. Phys. Chem. B*, 2005, **109**, 3519.
82. W. E. Acree, Jr., D. C. Wilkins, S. A. Tucker, J. M. Griffin and J. R. Powell, *J. Phys. Chem.*, 1994, **98**, 2537.
83. K. A. Fletcher, S. N. Baker, G. A. Baker and S. Pandy, *New J. Chem.*, 2003, **27**, 1706.
84. J. Kagimoto, K. Noguchi, K. Murata, K. Fukumoto, N. Nakamura and H. Ohno, *Chem Lett.*, 2008, **37**, 1026.
85. H. Every, A. G. Bishop, M. Forsyth and D. R. MacFarlane, *Electrochim. Acta*, 2000, **45**, 1279.

86. A. Stoppa, R. Buchner and G. Hefter, *J. Mol. Liq.*, 2010, **153**, 46.
87. M. Egashira, M. Nakagawa, L. Watanabe, S. Okada and J. I. Yamaki, *J. Power Sources*, 2005, **146**, 685.
88. A. Jarosik, S. R. Krajewski, A. Lewandowski and P. Radzimski, *J. Mol. Liq.*, 2006, **123**, 43.
89. M. Egashira, S. Okada and J. Yamaki, *Solid State Ionics*, 2002, **148**, 457.
90. S. H. Lee, S. H. Ha, N. M. Hiep, W. J. Chang and Y. M. Koo, *J. Biotechnol.*, 2008, **133**, 486.
91. A. Arce, M. J. Earle, S. P. Katdare, H. Rodríguez and K. R. Seddon, *Chem. Commun.*, 2006, 2548.
92. A. Arce, M. J. Earle, S. P. Katdare, H. Rodríguez and K. R. Seddon, *Fluid Phase Equilibria*, 2007, **261**, 427.
93. A. Arce, M. J. Earle, S. P. Katdare, H. Rodríguez and K. R. Seddon, *Phys. Chem. Chem. Phys.*, 2008, **10**, 2538.
94. S. Wellens, B. Thijs, C. Möller and K. Binnemans, *Phys. Chem. Chem. Phys.*, 2013, **15**, 9963.

# Chapter 2

## Improvement of miscibility between hydrophobic ionic liquids and hydrophilic ionic liquids by zwitterionization of a hydrophobic ionic liquid

# 2-1 Introduction

ILs are novel liquid materials with great potential for use in a variety of fields. Their chemical and physical properties are tunable by appropriate choice and design of cation and anion. A wide variety of ILs has now been prepared through modification of their cations and anions. However, there should be an upper limit to developing ILs with desired functions and properties by only designing their component ions.

An easy way to control the chemical and physical properties of ILs is to mix two or more ILs.[1] Mixing miscible ILs is useful for preparing monophasic IL systems with successively tuned chemical and thermal properties.[2] However, there is always a fear of the ion exchange reaction among the mixed ions that would lead to unexpected change in the physicochemical properties of pristine ILs.[3] To overcome this problem, the author has focused on zwitterions.[4] Zwitterions should prevent ion exchange in ILs, because their component cations and anions are both covalently tethered.[5] The combinations of ILs having significantly different ion structures provide biphasic IL systems. For example, $[P_{66614}]Cl$ and $[C_nmim]Cl$ ($n < 6$) form such biphasic systems.[6] This system do not combine properties and functions of each IL. There is an upper limit to control a phase behavior of IL mixtures by simple mixing of ILs.

The author's aim here is to present a strategy to combine two immiscible ILs, hydrophobic and hydrophilic ILs. For combining two immiscible ILs, the author focused on the use of a hydrophobic zwitterion having a hydrophilic anion (Figure 2-1). This zwitterion is expected to show miscibility with hydrophilic ILs. As a zwitterion the author chose 4-(tri-n-octylphosphonio)butanesulphonate (**1**), because it has two incompatible ions; a hydrophobic phosphonium cation and a hydrophilic sulfonate anion. As a hydrophilic IL the author used 1-ethyl-3-methylimidazolium leucine (**2**).

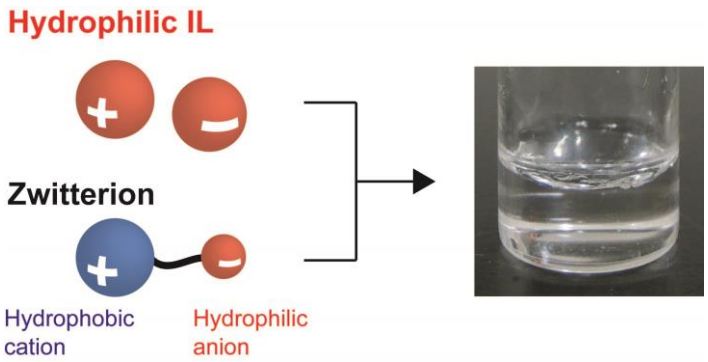


**Figure 2-1** Schematic illustration of the ion design in this chapter.

## 2-2 Results and discussion

### 2-2-1 Phase behavior of the mixtures of a phosphonium-type zwitterion and a hydrophilic ionic liquid

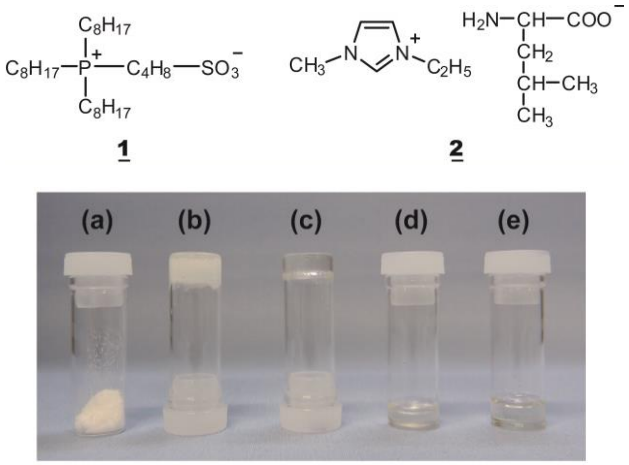


**Figure 2-2** Structure of the phosphonium-type zwitterion **1** and the amino acid IL **2** used in this experiment. Photograph of the mixtures of **1** and **2**. (a) **1** pristine in the solid state, (b) **1**/**2** mixture (mole fraction 0.50 for **2**) as the turbid gel, (c) **1**/**2** mixture (mole fraction 0.75 for **2**) as the translucent gel, (d) **1**/**2** mixture (mole fraction 0.83 for **2**) in the homogeneous liquid state, (e) **1** pristine in the liquid state.

**1**/**2** mixtures showed gel properties depending on the concentration of **1** in the mixtures (Figure 2-2). For example, **1**/**2** mixture (molar fraction 0.75 for **2**) formed a translucent gel. The resultant gels exhibited the Tyndall phenomenon when a laser (532 nm) was passed through them (Figure 2-3), indicating the formation of dispersed nano- or micro-particles in the gels. It is likely that the dispersed particles are formed through the aggregation of **1**. On the other hand, the mixtures containing a smaller amount of **2** than **1**/**2** mixture (mole fraction 0.50 for **2**) turned turbid following the precipitation of **1**. In contrast, the mixtures containing a larger amount of **2** than **1**/**2** (mole fraction 0.83 for **2**) mixture formed transparent liquids in which no light scattering was observed. These results revealed that the aggregation behavior of **1** in **2** is quite sensitive to the concentration of **1**. It is supposed that the formation of **1** aggregates plays an important role in inducing the gelation of **2**.

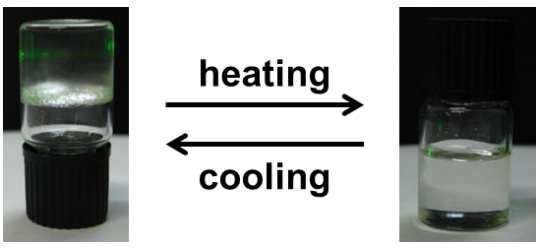


**Figure 2-3** Photograph of the Tyndall phenomenon for **1**/**2** mixture (mole fraction 0.75 for **2**).

## 2-2-2 Analysis of phase behavior of zwitterion/hydrophilic ionic liquid mixtures

### Wide-angle X-ray diffraction (WAXD) measurements

Wide-angle X-ray diffraction (WAXD) measurements were made on the mixtures (Figure 2-4). Several diffraction peaks were observed for **1**/**2** mixtures in the gel states. These diffraction peaks are ascribed to nano-ordered structures in the dispersed particles. In particular, the peaks at 16.7, 8.3, and 5.5 Å with a reciprocal d-spacing ratio of 1 : 2 : 3 indicate the formation of well-ordered layer structures with a layer thickness of 16.7 Å. Since the layer structure is similar to pristine **1** in the crystalline state, the author assumed that the dispersed particles should be formed by the aggregation of **1** in **2**. In view of the molecular structure of **1**, it is considered that **1** aggregates into a bilayer structure, consisting of alternating layers of hydrophobic and hydrophilic domains.[7]

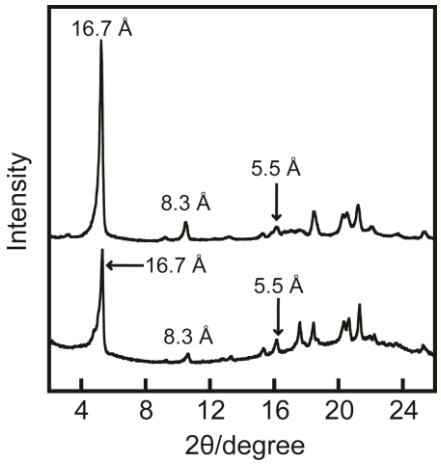


**Figure 2-4** X-ray diffraction patterns for: (a) **1** alone and (b) **1**/**2** mixture (mole fraction 0.75 for **2**) at 25 ˚C.

### Differential scanning calorimetry (DSC) measurement

**Table 2-1** Thermal properties of **1**, **2** and **1**/**2** mixtures on heating.

| Compound | Transition[a] | Temperature[b]/ºC | ΔH/J/g$^{-1}$ |
|---|---|---|---|
| **1** | Cr → Cr' | 54 | 3.2 |
| | Cr → L | 152 | 33 |
| **2** | G → L | −47 | — |
| **1**/**2**(mole fraction 0.75 for **2**) | G → Gel | −50 | — |
| | Gel → L | 55[c] | 16 |
| **1**/**2**(mole fraction 0.83 for **2**) | G → L | −47 | — |

[a] Abbreviations: Cr, Cr', crystalline phases; G, glass; L, liquid, —, not detected. [b] Onset temperature. [c] Temperature at the peak.

As expected, these gels showed thermotropic phase changes. The gel sample of **1**/**2** mixture (mole fraction 0.75 for **2**), for instance, becomes a transparent liquid at around 55 °C on heating. The obtained transparent liquid shows no Tyndall phenomenon. This suggests that the dispersed **1** particles disaggregate above the gel–liquid transition temperature. These results confirm that the aggregation of **1** induces the gelation of **2**. To gain further insight into the aggregation of **1**, the author performed differential scanning calorimetry (DSC) measurements for **1**, **2** and their mixtures (Table 2-1). The DSC thermogram of **1** shows two endothermic peaks at 54 and 152 °C on heating, which correspond to crystal–crystal' and crystal'–liquid transitions, respectively. The crystal–crystal' transition is attributed to the conformational melting of alkyl chains[8] on the phosphonium cation of **1**. The crystal'–liquid transition is attributed to the melting of the densely-packed zwitterionic parts. On the other hand, **2** shows only a glass transition at 47 °C. Based on these thermal properties of **1** and **2**, the author will discuss the phase behavior of **1**/**2** mixtures. For **1**/**2** mixture (mole fraction 0.75 for **2**), an endothermic peak corresponding to the gel–liquid transition was observed at 55 °C; this is roughly consistent with the crystal–crystal' transition temperature of **1**. It suggests that hydrophobic interaction between the alkyl chains of **1** is important in the aggregation of **1** in **2**. **1**/**2** mixture (mole fraction 0.83 for **2**) exhibited only a glass transition temperature as well as **1** pristine. These results verify that the concentration of **1** in the mixtures strongly influences the aggregation behavior of **1** in **2**. The dependence of concentration on the aggregation behavior can be explained by the interaction of **1** with **2**.

## NMR measurements

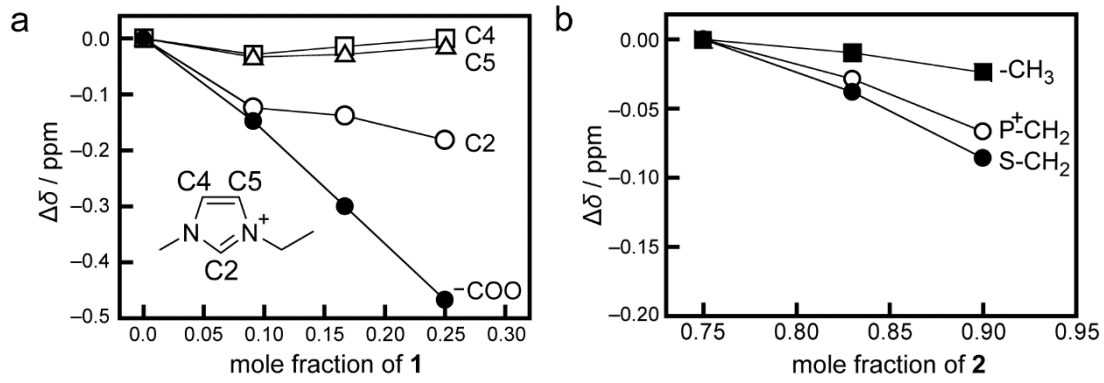


**Figure 2-5** $^{13}$C NMR chemical shift changes of (a) **2** through the addition of **1** and (b) **1** through the further addition of **2** into **1**/**2** mixture (mole fraction 0.75 for **2**) at 30 °C.

To clarify the ion pair state, the author studied the interaction between **1** and **2** by $^{13}C$ NMR measurements. $^{13}C$ NMR measurements are a useful method for examining the interaction among organic ions.[9] Measurements on the mixtures in the bulk state were performed by using coaxial capillary at 30 °C. Figure 2-5a shows the chemical shift changes of individual carbon atoms on the imidazolium cation and the leucine anion as a function of the mole fraction of **1**. The $^{13}C$ signal of the carbon at the second position of the imidazolium ring (C2) showed a shift to the higher magnetic field side with increasing **1** concentration, although the carbons at the fourth and fifth positions on the imidazolium ring (C4, C5) were only slightly influenced by the addition of **1**. The addition of **1** may increase the electron density at the C2 atom following the formation of hydrogen bonding between the proton on C2 (C2–H) and **1**. However, the signal from the carboxylate group (–COO) of the leucine anion also showed a shift to the higher magnetic field side, indicating a weakening of hydrogen bonding between the carboxylate group and C2–H. To confirm the formation of hydrogen bonding between C2–H and **1**, the author examined the $^{13}C$ chemical shift of **1** upon adding **2** to **1**/**2** mixture (mole fraction 0.75 for **2**) (Figure 2-5b). The $^{13}C$ signal of the carbon next to the phosphonium cation ($P^+$–$CH_2$) underwent a larger change than that of the carbon atom at the periphery of the long alkyl chains (–$CH_3$). These results indicate that the counter anion of the phosphonium cation is substituted by a softer anion than the sulfonate anion. The $^{13}C$ signal of the carbon atom next to the sulfonate group (S–$CH_2$–) also shifted to the higher magnetic field side. This chemical shift change can be explained by protonation of the sulfonate anion through the formation of hydrogen bonding with the imidazolium cation. These results reveal that the phosphonium cation of **1** prefers the leucine anion than its intrinsic anion, the sulfonate anion.

## FT-IR measurements

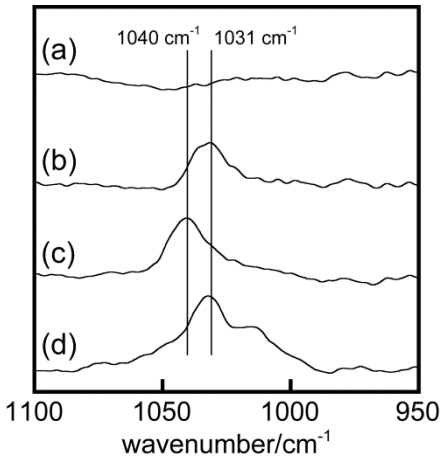


**Figure 2-6** IR spectra of (a) **2**, (b) **1**/**2** mixture (mole fraction 0.50 for **2**), (c) **1** and (d) imidazolium type zwitterion (3-(1-methyl-3-imidazolio)propanesulfonate) at room temperature.

FT-IR measurements for the mixtures further indicated the preferential interaction between the sulfonate anion and the imidazolium cation (Figure 2-6). In the FT-IR, pristine **1** showed the stretching vibration band ($\nu_{S=O}$) for the sulfonate group of **1** at 1040 $cm^{-1}$. Upon adding **2** it shifted to 1031 $cm^{-1}$. The situation is similar to $\nu_{S=O}$ for an imidazolium type zwitterion (3-(1-methyl-3-imidazolio)propanesulfonate) at 1032 $cm^{-1}$, suggesting that the sulfonate group of **1** preferentially interacts with the imidazolium cation in the mixture. The author believes that substitution of ion partners between **1** and **2** is important in promoting the solvation of **1** in **2**.

Based on the above results, the author concludes that the gelation of **1**/**2** mixtures is induced by two competing effects. One is the aggregation effect of **1** in **2** through the hydrophobic interaction between the long alkyl chains of **1**, and the other is the solvation effect of **2** for **1** through the preferential interaction between the sulfonate anion of **1** and C2–H of **2**. It is likely that competition between the two effects results in the formation of dispersed particles. In general dispersion particle gel systems, it is recognized that the interaction between dispersed particles and surrounding media is crucial in inducing gelation.[3] In our mixture, it is considered that the interaction of **2** with the surface of the **1** particles results in the gelation reducing the microscopic viscosity.

## 2-2-3 Ionic conductivity measurements of zwitterion/hydrophilic ionic liquid mixtures

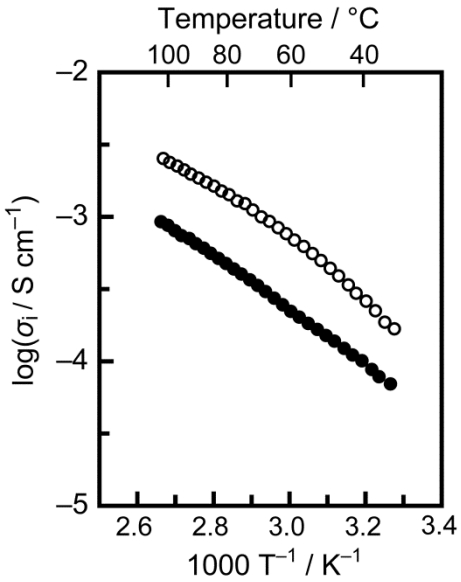


**Figure 2-7** Ionic conductivity of liquid state **2** (○) and gel state **1**/**2** mixture (mole fraction 0.75 for **2**) (●) on heating.

To analyze the effect on ion mobility upon adding **1**, the author measured ion conductivity for **2** and **1**/**2** mixture (mole fraction 0.75 for **2**) (Figure 2-7). For both samples the ionic conductivity increases with increasing temperature. The ionic conductivity of **1**/**2** mixture (mole fraction 0.75 for **2**) is about three times less than that of **2**. For example, the value for **1**/**2** mixture (mole fraction 0.75 for **2**) at 40 °C in the gel state was $1.01\times10^{4}$ S cm$^{-1}$ at 40 °C, and that for **2** at the same temperature was $2.60\times10^{4}$ S cm$^{-1}$. The decrease of ionic conductivity upon adding **1** may be due to the loss of macroscopic fluidity as a result of gelation.

The author determined the activation energy for these materials using the Vogel–Fulcher–Tamman (VFT) equation.[10] (Table 2-2) The activation energy for **1**/**2** mixture (mole fraction 0.75 for **2**) in the gel state is 5.34 keV, which is almost the same as that for **2** (5.37 keV). This similarity implies that **2** maintains its ion pair even after the addition of **1**, owing to the topologically tethered ionic structure of **1**.

**Table 2-2** VFT parameters for **2** and **1**/**2** mixture (mole fraction 0.75 for **2**).

| compound | $T_0$(K) | $A$(S/cm) | $B$(K) | $E_a$(keV)[a] | $R^2$ |
|---|---|---|---|---|---|
| **2** | 209 | 2.688 | 657 | 5.37 | 0.9995 |
| **1**/**2** mixture (mole fraction 0.75 for **2**)[b] | 198 | 0.516 | 654 | 5.34 | 0.9990 |

*A*: carrier ion number, *B*: activation energy [a]$E_a$ = B× 8.1674 ($10^5$ eV), [b]gel state

## 2-3 Conclusions

A binary system of a hydrophobic phosphonium-type zwitterion (**1**) and a hydrophilic amino acid IL (**2**) has been prepared. **1**/**2** mixtures exhibited gel or homogeneous liquid state depending on the concentration of **2**. The mixture forms gel states thermotropically through the dispersed aggregation of the phosphonium-type zwitterion. The dispersed particles are produced by the two competing effects: the aggregation effect of **1** through hydrophobic interaction, and the solvation effect of **2** for **1** through electrostatic interaction and hydrogen bonding. The activation energy of this gel-forming **1**/**2** mixture is almost the same as for **2**. This result indicates that the micro-segregation state can maintain their original mobility of the hydrophilic IL even after the addition of ZI. Increasing the mole fraction of **2** to over 0.75, the mixture forms a homogeneous liquid. Despite of the incompatibility between the phosphonium cation of **1** and the imidazolium cation of **2**, **1**/**2** mixtures were obtained as homogeneous liquids owing to the compatibility of the sulfonate anion of **1** and hydrophilic IL **2**. These results suggested that the zwitterionization of ILs is an effective strategy to improve the miscibility between hydrophilic and hydrophobic ILs.

# 2-4 Experiments

## Materials

Tri-*n*-octylphosphine, 1,4-butanesultone, 1,3-propanesultone and 1-methylimidazole were purchased from Tokyo Chemical Industry, Co. Ltd. Bromoethane and L-Leucine were purchased from Wako Chem. Co. 1-Methylimidazole was dried over KOH and distilled before use. All other commercially available chemicals were used as received.

## Synthesis of zwitterions and an IL

Syntheses of zwitterions and an IL used in this study are described below. The characterization of these compounds was performed by $^1$H NMR (α-400, JEOL), ESI-MS and elemental analysis.

**4-(Tri-*n*-octylphosphonio)butanesulphonate (1)**

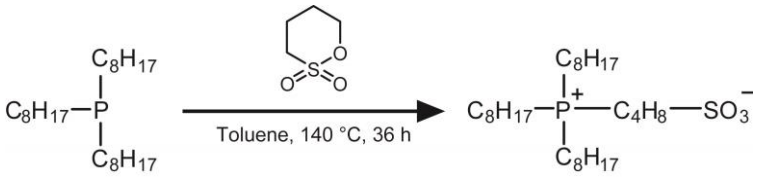


**1** was synthesized as reported previously.[11] To a solution of tri-*n*-octylphosphine (25.0 g, 67.5 mmol) in toluene (40 mL) was added a solution of 1,4-butanesultone (9.18 g, 67.5 mmol) in toluene with stirring at room temperature. The solution was heated and stirred at 140 °C for 36 h during which time a crude product was gradually obtained as a white precipitate. The resultant precipitate was collected via vacuum filtration, rinsed with diethyl ether. The crude material was further purified by recrystallization from ethyl acetate/methanol mixture (200 mL), to give 26.3 g (77%) as a white powder.

$^1$H NMR (400 MHz, $CDCl_3$, $\delta$/ppm relative to TMS): 0.89 (t, $J$ = 6.8 Hz, 9H), 2.22–1.30 (m, 24H), 1.48–1.50 (m, 12H), 1.72–1.79 (m, 2H), 1.97–2.05 (m, 2H), 2.22–2.25 (m, 6H), 2.43–2.50 (m, 2H), 2.87 (t, $J$ = 7.8 Hz, 2H). ESI–TOF–MS: calculated for $C_{28}H_{59}O_3PS$ $[M + Na]^+$: m/z = 529.80; found: 529.24. Elemental analysis: calculated for $C_{28}H_{59}O_3PS$: C, 66.36; H, 11.73; O, 9.47; P, 6.11; S, 6.33. Found: C, 66.32; H, 12.06; N, 0%.

**1-Ethyl-3-methylimidazolium leucine (2)**

**2** was synthesized as reported previously.[12] A solution of 1-ethyl-3-methylimidazolium bromide (8 g, 41.9 mmol) in water (200ml) was passed through a column filled with anion exchange resin (Amberlite IRN-78) to give a solution of 1-ethyl-3-methylimidazolium hydroxide. To the resultant solution was dropwise added L-leucine (6.0 g, 46.05 mmol) over a period of 30 min, and the resulting solution was stirred for 2 h at room temperature. The reaction mixture was evaporated under reduced pressure. To this crude material was added acetonitrile/methanol mixture, and it was stirred vigorously. The solution was then filtered to remove excess leucine. The acetonitrile/ methanol were removed by evaporation and the resulting liquid was dried under vacuum at 60 ºC for 12 h. The resultant product was obtained as a colorless liquid.

$^1$H NMR(400MHz, DMSO-$d_6$, $\delta$/ppm relative to TMS): 0.76 (d, $J$ = 7.2 Hz, 3H), 0.80 (d, $J$ = 6.4 Hz, 3H), 0.97-1.04(m, 1H), 1.34-1.40 (m, 4H), 1.62-1.69 (m, 1H), 2.73 (q, $J$ = 13.6 Hz, 1H), 3.84 (s, 3H), 4.20 (q, $J$ =34.0 Hz, 2H), 7.73 (1H, s), 7.82 (1H, s), 9.90 (1H,s).

Mixtures of **1** and **2** were prepared by slow evaporation of the methanol solution of **1** and **2**, and the obtained mixtures were further dried at 60 ºC under vacuum for 24 h.

**3-(1-methyl-3-imidazolio)propanesulfonate**

3-(1-Methyl-3-imidazolio)propanesulfonate was synthesized as reported previously.[13] To a solution of 1-methylimidazole in acetone was added a solution of 1,3-propanesultone in acetone with stirring under dry nitrogen at room temperature for 24 h. The resultant precipitate was separated by filtration. The resultant product was obtained as a white powder.

$^1$H-NMR (400MHz, $D_2O$, $\delta$/ppm relative to TMS): 2.32 (m, $J$ = 14.7 Hz, 2H), 2.92 (t, $J$ = 7.3 Hz, 2H), 3.90 (s, 3H), 4.37 (t, $J$ = 14.2 Hz, 2H), 7.46 (s, 1H), 7.53 (s, 1H), 8.76 (s, 1H). Elemental analysis: calculated for $C_7H_{12}N_2O_3S$: C, 41.16; H, 5.92; N, 13.72; O, 23.50; S, 15.70. Found: C 41.64; H 6.09; N 13.86%.

### Measurement

$^{13}C$ NMR spectra were recorded on a JEOL 400 spectrometer. Mixtures were loaded under a dry $N_2$ atmosphere into the internal chamber of a NMR coaxial capillary. The internal chamber was sealed by gas burner. The internal tube inserted a solution of DMSO-$d_6$ in the external chamber. The insert was sealed by gas burner. DSC measurements were performed on a DSC6220 (SEIKO Instrument Inc.) at a scanning rate of 5 ºC $min^{-1}$. X ray diffraction measurements were performed on a Smart Lab (Rigaku). Samples were loaded into 1 mm capillaries and sealed by bas burner to prevent water absorption. Ionic conductivity was measured by the AC impedance method using a Schlumberger Solartron 1260 impedance/gain-phase analyzer. The impedance of the samples was measured from 10 Hz to 1 MHz with temperature scanning at 2 °C $min^{-1}$ from 30 to 110 °C.

## 2-5 References


1. H. Niedermeyer, J. P. Hallett, I. J. Villar-Garcia, P. A. Hunt and T. Welton, *Chem. Soc. Rev.*, 2012, **41**, 7780.
2. (*a*) J. Kagimoto, K. Noguchi, K. Murata, K. Fukumoto, N. Nakamura and H. Ohno, *Chem. Lett.*, 2008, **37**, 1026; (*b*) J. N. C. Lopes, T. C. Cordeiro, J. Esperanca, H. J. R. Guedes, S. Huq, L. P. N. Rebelo and K. R. Seddon, *J. Phys. Chem. B*, 2005, **109**, 3519; (*c*) P. Navia, J. Troncoso and L. Romani, *J. Solution Chem.*, 2008, **37**, 677.
3. J. Kagimoto, N. Nakamura, T. Kato and H. Ohno, *Chem. Commun*., 2009, 2405.
4. Y. Ito, Y. Kohno, N. Nakamura and H. Ohno, *Chem. Commun*., 2012, **48**, 11220.
5. M. Yoshizawa, M. Hirao, K. Ito-Akita and H. Ohno, *J. Mater. Chem.*, 2001, **11**, 1057.
6. A. Arce, M. J. Earle, S. P. Katdare, H. Rodríguez and K. R. Seddon, *Chem. Commun.*, 2006, 2548
7. K. F. Ma, K.M. Lee, L. Minkova and R. G. Weiss, *J. Org. Chem.*, 2009, **74**, 2088.
8. C. M. Gordon, J. D. Holbrey, A. R. Kennedy and K. R. Seddon, *J. Mater. Chem.*, 1998, **8**, 2627.
9. (*a*) A. G. Avent, P. A. Chaloner, M. P. Day, K. R. Seddon and T. Welton, *J. Chem. Soc., Dalton Trans.*, 1994, 3405; (*b*) J. Zhang, H. Zhang, J. Wu, J. Zhang, J. He and J. Xiang, *Phys. Chem. Chem. Phys.*, 2010, **12**, 1941.
10. (*a*) H. Vogel, *Phys. Z.*, 1921, **22**, 645; (*b*) G. S. Fulcher, *J. Am. Ceram. Soc.*, 1925, **8**, 339; (*c*) G. Tamman and W. Hesse, *Z. Anorg. Allg. Chem.*, 1926, **156**, 245.
11. S. Ueda, J. Kagimoto, T. Ichikawa, T. Kato and H. Ohno, *Adv. Mater.*, 2011, **23**, 3071.
12. K. Fukumoto, M. Yoshizawa and H. Ohno, *J. Am. Chem. Soc.*, 2005, **127**, 2398.
13. M. Galin, A. Chapoton and J.-C. Galin, *J. Chem. Soc., Perkin Trans. 2*, 1993, 545.

# Chapter 3

## Preparation of nano-segregated ionic liquid systems

# 3-1 Introduction

Recently, there has been increasing attention on binary or multicomponent systems of ILs because these systems have potential to function as a new matrix exhibiting novel properties, which is hard to be produced by a one-component IL system. In chapter 2, the author described a binary IL system forming thermotropic gel state by a suitably designing hydrophobic phosphonium-type zwitterion and a hydrophilic IL. The formation of the gel state is attributed to the micro-segregation of the phosphonium-type zwitterion. In addition, the micro-segregation state can maintain original mobility of the hydrophilic IL even after mixing of zwitterion.

The author's intention this chapter is to construct a novel binary IL system providing nano-biphasic states where two incompatible IL nano-domains coexist homogeneously in a macroscopic scale. (Figure 3-1) The author envisions that such a system has potential to open up a new strategy to combine two different ILs into a matrix keeping their original functions and properties. In this chapter, the author has intended to develop nano-segregated IL systems consisted of a hydrophilic IL and a hydrophobic IL.

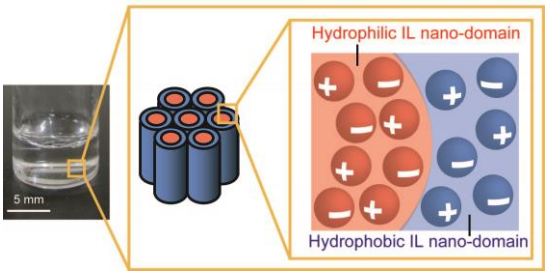


**Figure 3-1** Schematic illustration of a nano-biphasic IL system consisting of hydrophilic and hydrophobic IL nano-domains.

For realizing such systems, the author focused on lyotropic liquid crystal system.[1] Amphiphilic molecules are consisting of two immiscible parts, such as hydrophilic and hydrophobic parts, exhibit liquid crystalline (LC) phases through the segregation of hydrophilic and hydrophobic parts in the presence of suitable solvents such as water. The dimensional orders of nano-segregated structures are governed by the volume balance of the two immiscible parts as shown in Figure 3-2.[2] Smectic phases (layer structures) with flat interfaces between the nano-segregated regions of the two incompatible units result only for molecules where the incompatible segments have comparable cross section area. If the size of one segment is increased, then a curvature of these interfaces arises, which leads to the formation of columnar and cubic nano-segregated structures. For the construction of a nano-segregated structure consisting of a hydrophilic IL and a hydrophilic IL, the authors focused on the use of phosphonium-type zwitterions having a hydrophilic anion. They prefer to form homogeneous complexes with lithium bis(trifluoromethanesulfonyl) imide ($LiTf_2N$) forming two adjacent ion pairs: a hydrophobic ion pair and a hydrophilic ion pair.[3,4] These complexes are expected to show two conflicting properties: miscibility and immiscibility with hydrophilic ILs and form nano-segregated structures.

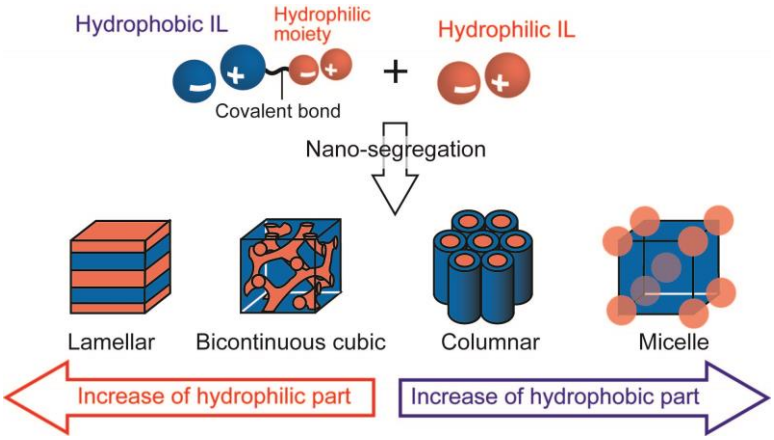


**Figure 3-2** Material design for the development of nano-segregated IL systems.

# 3-2 Results and discussion

## 3-2-1 Structure design of ionic liquids

### Design of hydrophobic ionic liquids having a hydrophilic moiety

Phosphonium-type ILs having a hydrophilic moiety **4**-**7** were designed and synthesized. When mix a phosphonium-type IL and an imidazolium-type IL, the mixtures formed two macro-separated phases because the structure of cations are considerably different.[5] The combination of a phosphonium cation having long alkyl chains (n > 5) and an amino acid anion which is relatively hydrophilic ion is gave the construction of biphasic state when mixing with water.[6] As a hydrophilic moiety, the author introduced ionic groups (sulfonate group, carboxylate group and phosphate group) and hydroxyl groups. It is expected that the mixture of an IL having a hydrophilic moiety in the phosphonium cation and a hydrophilic IL forms nano-segregated structures because the phosphonium cation shows two conflicting miscibility with the hydrophilic IL. One is miscibility with a hydrophilic group and a hydrophilic IL. The other is immiscibility with a hydrophilic phosphonium cation and a hydrophilic IL. Compound **4** was synthesized by quaternization of phosphine. Compound **4** was obtained as colorless liquid at room temperature. Compounds **5**-**7** were prepared by complexing zwitterions having a hydrophobic phosphonium cation and a hydrophilic anion (sulfonate, carboxylate or phosphate) with equimolar $LiTf_2N$. The resultant complexes are viscous liquids at room temperature. To examine the effect of the introduce of hydroxyl groups to the phosphonium cation on the nano-segregated behavior, tri-*n*-octylphosphonium bis(trifuoromethylsulfonyl)imide **3** was also prepared for comparison.

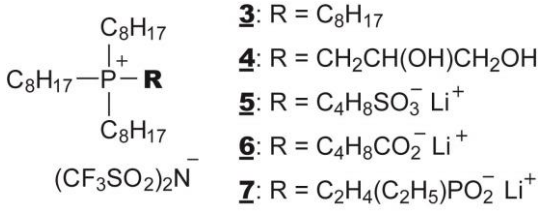


**Figure 3-3** Structure of phosphonium-type ILs having a hydrophilic moiety used in this chapter.

Design of hydrophilic ionic liquids

Water is an essential solvent for self-organization of amphiphilic molecules. When ILs use as an alternative solvent of water, the introduction of hydroxyl groups to the ion structure is one of the useful approaches.[7] Therefore, the author designed and synthesized tris(2-hydroxylethyl)-methylammonium bis(trifuoromethylsulfonyl)imide **8**, choline bis(trifuoromethylsulfonyl)imide **9** and 1-(2-hydroxyethyl)-3-methylimidazolium bis(trifuoromethylsulfonyl)imide **10**. To examine the effect of the introduce of hydroxyl groups to the cation on the nano-segregated behavior, 1-butyl-3-methylimidazolium bis(trifuoromethylsulfonyl)imide **11** was also prepared for comparison. As anion of hydrophilic ILs, the authors chose bis(trifuoromethylsulfonyl)imide anion to avoid the system become complicated.

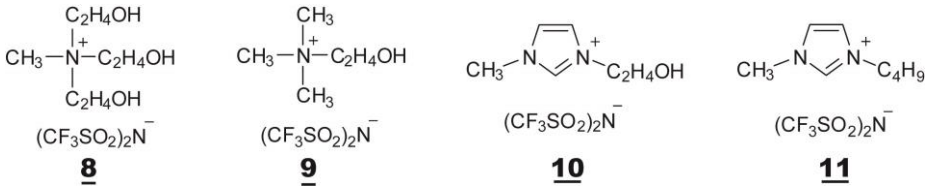


**Figure 3-4** Structure of hydrophilic ILs used in this chapter.

## 3-2-2 Thermal properties of hydrophobic ionic liquids having a hydrophilic moiety

The thermal properties of hydrophobic ILs having a hydrophilic moiety **3**-**7** were investigated by polarizing optical microscopy (POM), differential scanning calorimetry (DSC) and X-ray measurements. The phase transition temperatures and associated enthalpy values are shown in Table 3-1. Hydrophobic ILs **5**-**7** exhibit micellar cubic LC phase. Considering the cone-like molecular structure of phosphonium cation, it is likely that compounds **5**-**7** form nano-segregated LC structures in which the vertex of the cone gathers into spherical hydrophilic domains surrounded by the hydrophobic IL domain.[8] On the other hand, no LC property was observed for compounds **3**-**4**. The comparison of the thermal properties of these hydrophobic ILs indicates that the introduction of the ion group to the phosphonium cation plays an important rule for the aggregation behavior of these hydrophobic ILs. The phase transition temperatures of these compounds are influenced by the structure of ions. For example, the phase transition temperature from cubic phase to isotropic phase of compound **5** is 198 ºC, which is considerably higher than that of compound **7** is 41 ºC. Compound **6** having carboxylate group in phosphonium cation exhibits a cubic phase from 10 to 200 ºC as well as compound **5**. These results suggest that it is important to design the anion structure on the cation for forming the LC properties.

**Table 3-1** Thermal properties of phosphonium-type ILs having a hydrophilic moiety **3**-**7**.

| Compound | Phase transition behavior[a]/°C | | | | | | |
|---|---|---|---|---|---|---|---|
| **3** | G | −60 | Iso | | | | |
| **4** | G | −67 | Iso | | | | |
| **5** | G | −13 | Cub | 179 (0.37) | Cub | 198 (0.45) | Iso |
| **6** | Cr | 10 (7.07) | Cub | 200 (0.55) | Iso | | |
| **7** | G | −31 | Cub | 41 (0.79) | Iso | | |

G, Glass; Cr, Crystalline; Cub, cubic; Iso, Isotropic. [a]Transition temperatures (°C) and enthalpy changes (kJ/mol, in parentheses) are determined by DSC on the second heating.

## 3-2-3 Nano-segregated behavior of mixtures **3**-**7** and **8**

Hydrophobic ILs having a hydrophilic moiety **3**-**7** were mixed with hydrophilic IL **8** in various molar ratios. The miscibility of the two ILs and the induced LC phases for the mixtures are summarized in Table 3-2. The phosphonium-type ILs having a ionic moiety **5**-**7** formed homogeneous mixture with IL **8**, while compounds **3**-**4** show no miscibility with IL **5**. These results suggested that the compatibility of hydrophobic ILs having a hydrophilic moiety with hydrophilic IL **8** is enhanced by introduction of the ionic moiety. On the other hand, the introduction of hydroxyl groups is not useful for increase the compatibility with a hydrophilic IL.

The homogeneous mixtures of hydrophobic ILs **5**-**6** and hydrophilic IL **8** show thermotropic LC phases. It is notable that the mixtures of **5** and **8** showed not only cubic but also columnar phase depending on the composition of hydrophobic IL **5** and hydrophilic IL **8**. In the below, the author discuss the effect of the ion structure of hydrophobic ILs **3**-**6** and the effects of ion structures of hydrophilic IL **8** on the nano-segregated behavior of mixtures.

**Table 3-2** The miscibility of phosphonium-type ILs having a hydrophilic moiety **3**-**7** and hydrophilic ammonium-type IL **8** and the induced nano-segregated structures for the obtained mixtures.

| Hydrophobic IL | Structure of X | The miscibility phosphonium-type ILs **3**-**7** and hydrophilic IL **8** |
|---|---|---|
| **3** | $C_8H_{17}$ | Immiscible |
| **4** | $CH_2CH(OH)CH_2OH$ | Immiscible |
| **5** | $C_4H_8SO_3^-Li^+$ | Miscible (induced LC phase) |
| **6** | $C_4H_8CO_2^-Li^+$ | Miscible (induced LC phase) |
| **7** | $C_2H_4(C_2H_5)PO_2^-Li^+$ | Miscible |

## Nano-segregated properties of mixture of phosphonium-type ionic liquid **5** and ammonium-type ionic liquid **8**

It is interested that the mixtures of **5** and **8** (**5**/**8** mixture) form micellar cubic and columnar LC structures depending on the ratio of the components between hydrophilic IL **5** and hydrophobic IL **8**. **5**/**8** mixtures form micellar cubic structures when the mole fraction of **8** is below 0.35. The increase of composition ratio of **8** in the mixtures induced the formation of columnar structures. Characterization of a micellar cubic phase was performed by small angle X-ray scattering (SAXS) measurements. For example, the SAXS pattern of **5**/**8** mixture (mole fraction 0.35 for **8**) at 60 ºC shows three intense peaks at 3.16 (27.9 Å), 3.41 (25.8 Å) and 3.75 (23.5 Å) and two weak peaks at 4.48 (19.7 Å) and 5.88 (15.0 Å) (Figure 3-5). The reciprocal *d*-spacing ratio of the five peaks is √4 : √5 : √6 : √8 : √14, which can be assigned to the (200), (210), (211), (220) and (321) reflections of a cubic structure with the *Pm3n* symmetry. This result shows that mixture **5**/**8** (mole fraction 0.35 for **8**) forms the micellar cubic phase.

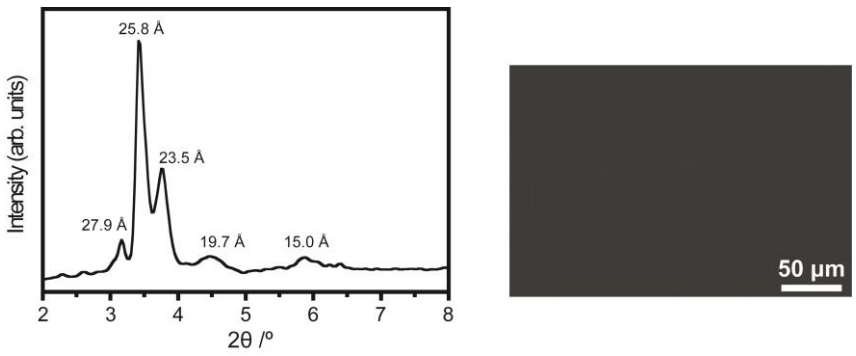


**Figure 3-5** Small-angle X-ray scattering pattern and polarizing optical micrograph of **5**/**8** mixture (mole fraction 0.35 for **8**) at 60 °C.

The columnar phases formed by **5**/**8** mixtures were also characterized by the Wide-angle X-ray diffraction (WAXD) measurement and polarizing optical microscopic (POM) observation (Figure 3-6). The WAXD pattern of **5**/**8** mixture (mole fraction 0.5 for **8**) at 30 ºC shows one intense peak at 3.78º (23.4 Å) and one weak peak at 5.98º (14.8Å) (Figure 3-6). The reciprocal *d*-spacing ratio of the two peaks is 1 : √3, which can be assigned to the (100) and (110) reflections of a hexagonal columnar structure with the *p6mm* symmetry. POM observation for **5**/**8** mixture (mole fraction 0.5 for **8**) further supports the formation of the columnar structure. This result shows that **5**/**8** mixture (mole fraction 0.5 for **8**) forms the columnar phase.

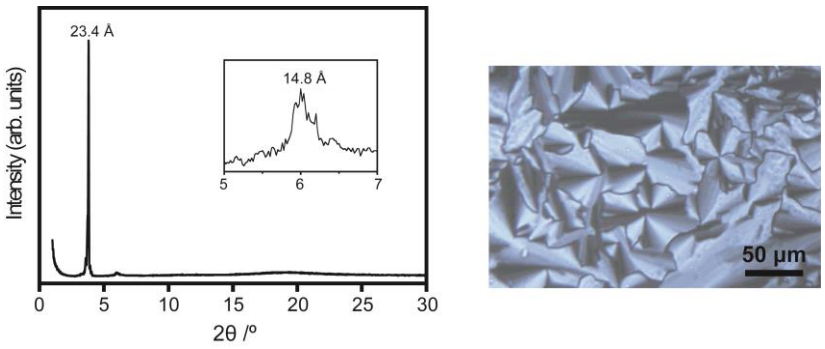


**Figure 3-6** Wide-angle X-ray diffraction pattern and polarizing optical micrograph of **5**/**8** mixture (mole fraction 0.5 for **8**) at 30 °C.

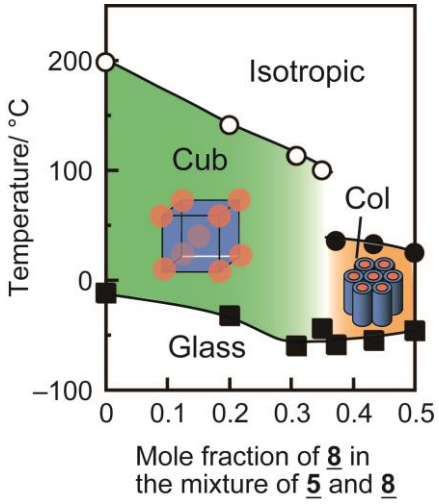


**Figure 3-7** Phase diagram of the mixtures of **5** and **8**.

The phase transition behavior for **5**/**8** mixtures is summarized in the diagram (Figure 3-7). The micellar cubic and columnar phases are observed in this order with the increase of the mole fraction of hydrophilic IL **8**. In the course of studies on self-organizing materials, it has been well-studied that amphiphilic molecules[9] and block copolymers[10] consisting of two or more immiscible parts form a variety of nano-segregated structures depending on the composition of the immiscible parts. These studies have revealed that the change of nano-segregated structures from discontinuous cubic to columnar is induced by increasing the volume fraction of inner components. This has been explained by the decrease of the interface curvature between hydrophobic and hydrophilic domains. This general insight further supports the author's conclusion that **5**/**8** mixtures form nano-segregated states consisting of hydrophilic inner domains and surrounding hydrophobic outer domains.

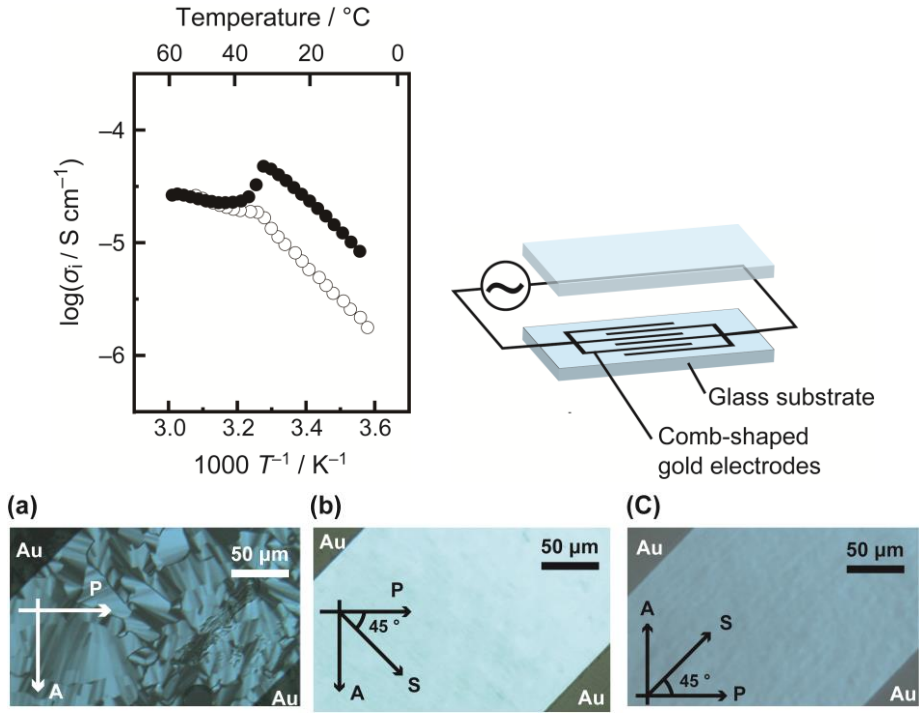


**Figure 3-8** Ionic conductivity of **5**/**8** mixture (mole fraction 0.37 for **8**) as a function of temperature upon heating. (●) and (○) indicate the ionic conductivity of **5**/**8** mixtures with aligned columnar structure parallel ($\sigma_{\parallel}$) and perpendicular ($\sigma_{\perp}$) to the electric field, respectively. Illustration of glass cell with comb-shaped gold electrodes for the ion conduction measurements. Polarizing optical microscopic images for **5**/**8** mixture (mole fraction 0.37 for **8**): (a) before shearing; (b) after shearing the sample parallel to the electric field, (c) after shearing the sample perpendicular to the electric field. The mechanical shearing makes cylindrical axis in the hydrophilic IL domains aligns to the shearing direction. Directions: A: analyzer; P: polarizer; S: shearing.

The formation of columnar structure has been also confirmed by their ion conduction behavior. Ion conduction measurements were performed for two samples of **5**/**8** mixture (mole fraction 0.37 for **8**) with macroscopically-aligned columnar structure parallel and perpendicular to the electric fields. Each result corresponds to the ionic conductivities parallel and perpendicular to the column axis, respectively. The alignment of columnar structure was induced by mechanical shearing.[11] Figure 3-8 shows the ionic conductivities of **5**/**8** mixture (mole fraction 0.37 for **8**) in the directions parallel ($\sigma_{\parallel}$) and perpendicular ($\sigma_{\perp}$) to the column axis. It is noteworthy that the values of $\sigma_{\parallel}$ are higher than those of $\sigma_{\perp}$. For example, **5**/**8** mixture shows conductivities of $\sigma_{\parallel} = 4.5 \times 10^{-5}$ S cm$^{-1}$ and $\sigma_{\perp} = 2.7 \times 10^{-5}$ S cm$^{-1}$ at 30 °C. It should be also noted that the difference of ionic conductivities between $\sigma_{\parallel}$ and $\sigma_{\perp}$ disappears upon the phase transition from the columnar phase to the isotropic liquid state. This ion conduction behavior can be adequately explained by a model in which the ions move smoothly in the direction parallel to the columnar axis without crossing the phase interfaces between two incompatible IL domains, while their migrations in the direction perpendicular to the column axis are disturbed by the phase interfaces.

## 3-2-4 Effects of the ion structures on the nano-segregated structures

### Effects of the hydrophilic groups in cation of phosphonium-type ionic liquids on the nano-segregated properties

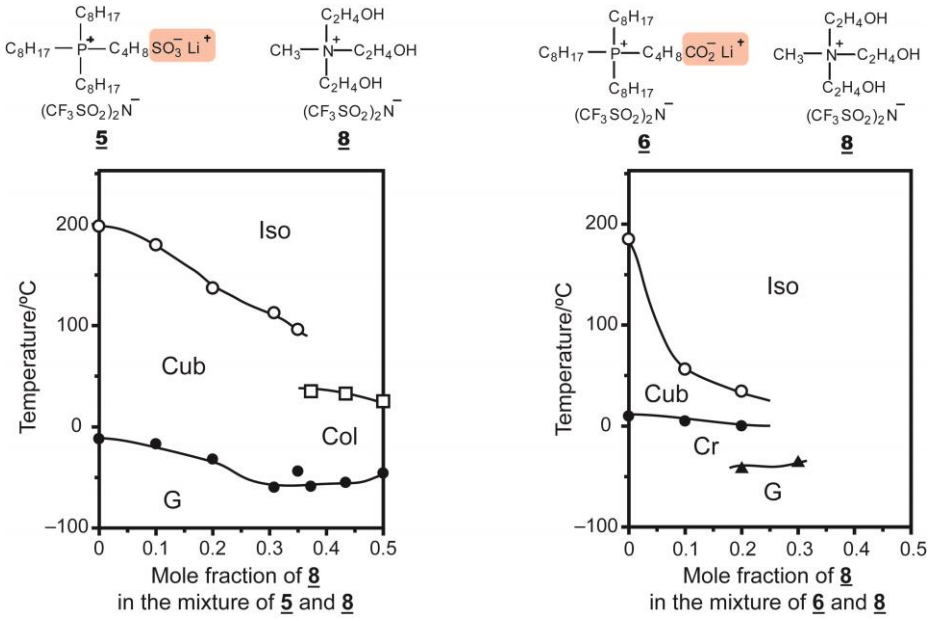


**Figure 3-9** The phase diagrams of **5**/**8** mixtures and **6**/**8** mixtures.

To examine the effects of the anion structure in phosphonium cation on the nano-segregated properties, the mixtures **5**/**8** and **6**/**8** were prepered and evaluated. The phase diagrams of mixtures **5**/**8** and **6**/**8** are shown in Figure 3-8. It should be pointed out that the columnar phases never obseved for **6**/**8** mixtures. The formation of the liquid crystallin phase is induced for **6**/**8** mixtures until the mole fraction of **8** reaches 0.2 while only an isotropic liquid state is observed when the mole fraction of **8** is over 0.3. The isotropization temperatures of **6**/**8** mixture are significantly lower than those of **5**/**8** mixture, despite the isotropization temperature of **5** and **6** is almost same. These results suggest that the stability of nano-segregated structuers is affeccted by the anion structure on the phosphonium cation.

### Effect of the structure of hydrophilic ionic liquids on the nano-segregate properties

Hydrophobic IL **5** having a sulfonate anion was mixed with hydrophilic ILs **8**-**11** in various molar ratios. The miscibility of the two ILs and the induced LC phases for the mixtures is summarized in Table 3-3. Hydrophilic ILs **8**-**10** formed homogeneous mixtures with hydrophilic IL **5**. The homogeneous mixtures of phosphonium type IL **5** and hydrophilic ILs **8**-**11** show LC phases. It is worthy of attention that the induction of columnar phases is exclusively for the mixture **5** and **8**. It is

well known that the nano-segregation structures are affected by the volume balance of the two immiscible parts. The change of nano-segregated structures from micellar cubic to columnar is induced by increasing the volume fraction of inner components. Considering the structure of phosphonium-type IL **5**, the inner component is hydrophilic part. In actually, the combination of **5** and water or glycerol induces the formation of columnar structures. It is expected that the hydrophilic structure of the tris(2-hydroxylethyl)methylammonium cation contributed the increase of inner volume because the ammonium cation having multiple hydroxyl groups shows higher compatibility with water than other cations.

**Table 3-3** The miscibility of phosphonium-type ILs having a hydrophilic moiety **5** and hydrophilic ILs **8-11** and the induced nano-segregated structures for the obtained mixtures

| Hydrophilic IL | 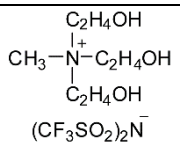 | 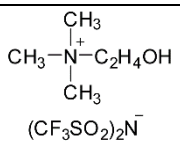 | 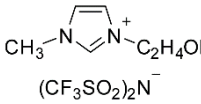 | 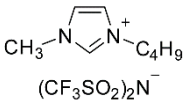 |
|---|---|---|---|---|
| | **8** | **9** | **10** | **11** |
| The LC phase of hydrophobic IL **5** and hydrophilic ILs | Cub, Col | Cub | Cub | Cub |

## Effects of the alkyl chain length of the phosphonium cation on the nano-segregated structures

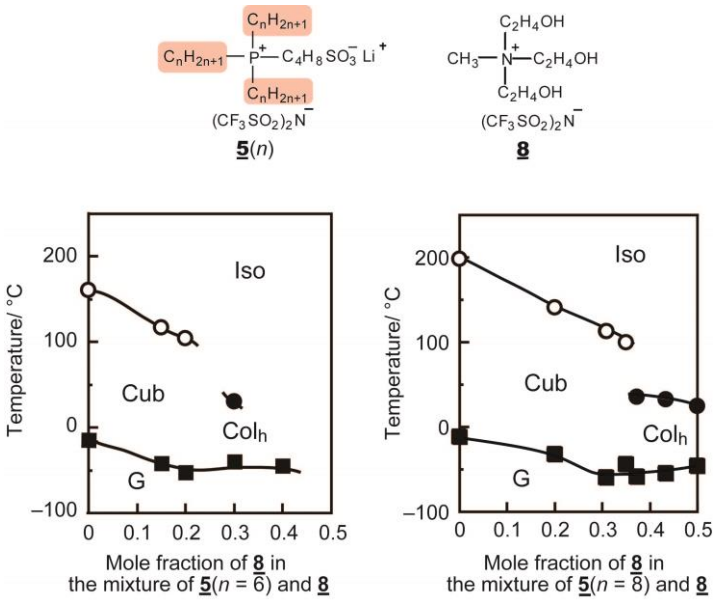


**Figure 3-10** The phase diagrams of **5**(*n*)/**8** mixtures.

The author has examined the effects of the alkyl chain length of the phosphonium cations on the phase behavior. The thermal behavior of **5**(*n*)/**8** mixtures (*n* = 6 or 8) is summarized in Figure 3-10. It can be seen that the thermal stability of the nano-segregated state decreases with the increase of the mole fraction of **8**. **5**(*6*)/**8** mixtures maintain the nano-segregated state in a temperature range higher than 100 °C when the mole fraction of **8** is below 0.2. The formation of the nano-segregated state is induced for **5**(*6*)/**8** mixtures until the mole fraction of **8** reaches 0.3 while only an isotropic liquid state is observed when the mole fraction of **8** is over 0.4. On the other hand, **5**(*8*) having longer alkyl chains form nano-segregated states even in the presence of equimolar **8**. Comparison of these two diagrams clearly shows that the nano-segregated state of **5**(*8*)/**8** mixtures is thermally more stable than those of **5**(*6*)/**8** mixtures. A plausible explanation of this difference is that the elongation of alkyl chains on the phosphonium cation, enhancing the hydrophobicity, stabilizes the nano-segregated state.

## Effects of the alkali metal ions on the nano-segregate properties

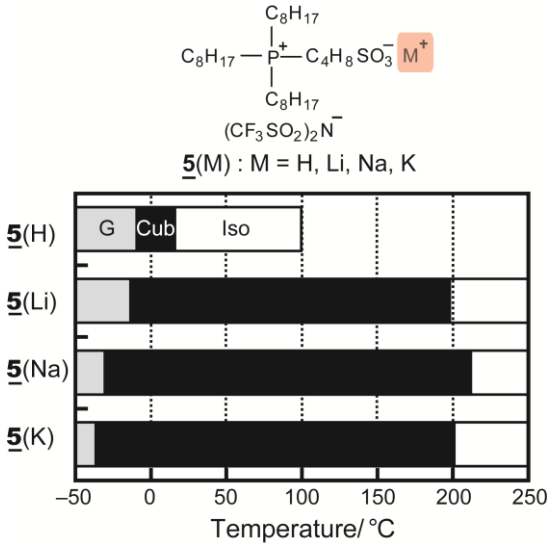


**Figure 3-11** Comparison of LC properties between a series of phosphonium-type ILs **5**(M). G: glassy, Cub: cubic phase, Iso: isotropic liquid.

Comparison of the thermal properties of among hydrophobic ILs having different alkali metal ions is shown in Figure 3-11. Hydrophobic ILs **5**(M) exhibit cubic LC phase. The phase transition temperatures of these compounds are influenced by the structure of ions. For example, the phase transition temperature from cubic phase to isotropic phase of compound **5**(Li) is 198 ºC, which is considerably higher than that of compound **5**(H) is 16 ºC. **5**(Na) exhibits cubic phase from −30 to 212 ºC as well as **5**(K). These results suggested that the ion pair ($SO_3$ anion/alkali metal cation) plays an important rule for the phase behavior of these hydrophobic ILs.

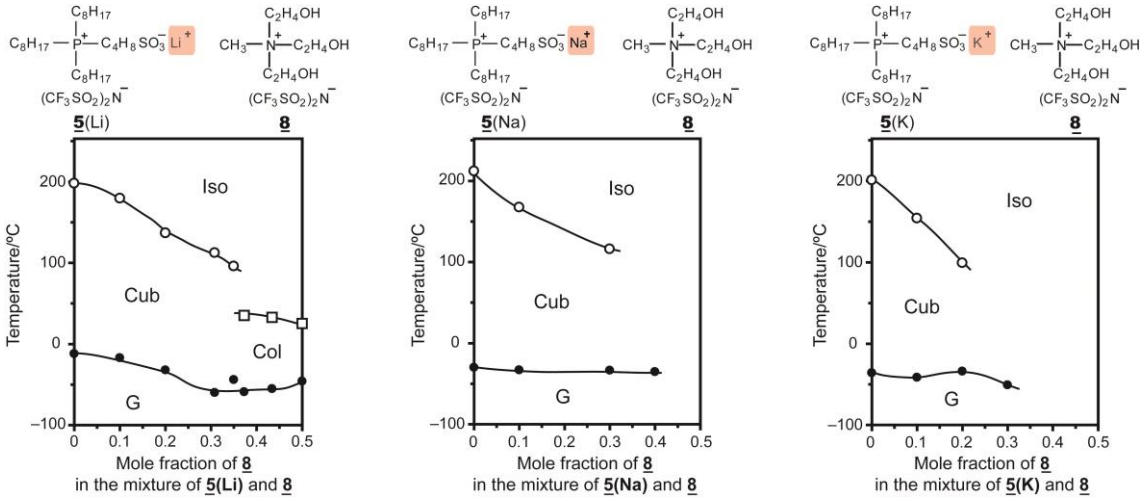


**Figure 3-12** The phase diagrams of **5**(M)/**8** mixtures.

To examine the effects of the alkali mehtal ion in hydrophobic ILs on the nano-segregated properties, the mixtures **5**(M)/**8** (M = H, Li, Na, K) were prepered and evaluated. The phase diagram of **5**(H)/**8** mixtures is not shown because no LC property was observed. The formation of the nano-segregated state is induced for **5**(Na)/**8** mixtures until the mole fraction of **8** reaches 0.3 while only an isotropic liquid state is observed when the mole fraction of **8** is over 0.4. **5**(K)/**8** mixtures show nano-segregated structure until the mole fraction for 0.2 for **8**. On the other hand, **5**(Li)/**8** mixtures having longer alkyl chains form nano-segregated states even in the presence of equimolar **8**. Comparison of these three diagrams clearly shows that the nano-segregated state of **5**(Li)/**8** mixtures is the most thermally stable in **5**(M)/**8** mixtures. A plausible explanation of this difference is that the decrease of ion radii of alkali metal ion, enhancing the electrostatic interaction, stabilizes the nano-segregated state.

## 3-3 Conclusions

The author has designed nano-segregated IL systems consisting of a hydrophilic IL and a hydrophilic IL. The nano-segregated systems have been prepared by mixing hydrophilic phosphonium-type ILs with a hydrophilic moiety and hydrophilic ILs. The phase behavior of these hydrophobic IL/hydrophilic IL mixtures depends on their ionic structures, and some mixtures show LC behavior due to the nano-segregation of their hydrophilic and hydrophobic parts. The nano-segregated structures are induced by the effects that the hydrophilic IL has good compatibility with the hydrophilic moiety in the hydrophilic IL while it is incompatible with the hydrophobic phosphonium cation. For example, a phosphonium-type IL with a sulfonate anion (**5**) forms homogeneous mixtures with an ammonium-type IL containing multiple hydroxyl groups (**8**) and the resultant mixtures showed two LC phases depending on the composition of the two components. Increasing the mole fraction of the hydrophilic IL in the mixture, the LC phases changed from a cubic structure to a columnar structure. These results indicate that the obtained nano-segregated structures consist of hydrophilic inner domains and a hydrophobic outer nano-domain. Moreover, their liquid crystallinity is found to be sensitive to the structure of a hydrophilic moiety on the phosphonium cation. The ion structure design using nano-segregated IL system will offer unique opportunity to expand potential application of ILs.

## 3-4 Experiments

### Materials

Tri-*n*-octylphosphine, tri-*n*-hexlyphosphine 1,4-butanesultone, tetra-*n*-octylphosphonium bromide, 5-bromovalerate, diethyl-2-bromoethylphosphonate and choline bromide were purchased from Tokyo Chemical Industry, Co. Ltd. Tris(2-hydroxyethyl)methylammonium methylsulfate, were purchased from Sigma Aldrich. 1-chloro-2,3-propanediol was purchased from Wako Chem. Co. 2-Bromoethanol and 1-butyl-3-methylimidazolium bis(trifluoromethylsulfonyl)imide (**11**) were purchased from Kanto chemical co., Inc. Lithium bis(trifluoromethylsulfonyl)imide was supplied from Sumitomo 3M Ltd. 1-Methylimidazole was dried over KOH and distilled before use. All other commercially available chemicals were used as received.

### Synthesis of zwitterions and ionic liquids

Syntheses of a zwitterion and ILs used in this study are described below. The characterization of these compounds was performed by $^{1}$H NMR (α-400, JEOL), ESI-MS and elemental analysis.

**Tetra-*n*-octylphosphonium bis(trifluoromethylsulfonyl)imide (3)**

To a solution of tetra-*n*-octylphosphonium bromide (5.0 g, 8.9 mmol) in dichloromethane (100 ml) was added a solution of lithium bis(trifluoromethylsulfonyl)imide ($LiTf_2N$) (2.8 g, 9.8 mmol) in water with stirring at room temperature. The solution was mixed at room temperature for 12 h, and the organic layer was separated and washed three times with water. The dichloromethane was removed by evaporation and the resulting liquid was dried under vacuum at 60 °C for 12 h. The resultant product was obtained as a colorless liquid.

$^1$H NMR (400MHz, $CDCl_3$, $\delta$/ppm relative to TMS): 0.88 (t, $J$ = 11.0 Hz, 12H), 1.30-1.32 (m, 32H), 1.43-1.54 (m, 16H), 2.07-2.13 (m, 8H). Elemental analysis: Calculated for $C_{34}H_{68}F_6NO_4PS_2$: C, 53.45; H, 8.97; F, 14.92; N, 1.83; O, 8.38; P, 4.05; S, 8.39. Found: C, 53.37; H, 9.00; N, 1.63%.

**Tri-*n*-octyl(2,3-dihydroxylpropyl)phosphonium bis(trifluoromethanesulfonyl)imide (4)**

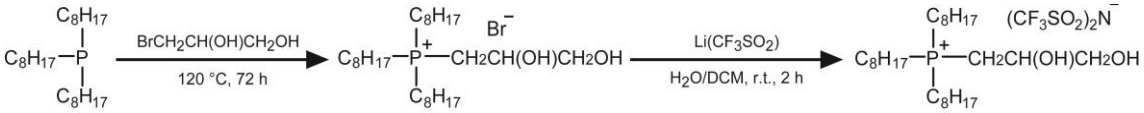


**4** was synthesized as reported previously.[12] The mixture tri-*n*-octylphosphine (6.10g, 16.5mmol) and 1-chloro-2,3-propanediol (2.0g, 18.1mmo) stirred at 120 °C for 72h. The reaction mixture was extract with diethyl ether and washed with water. The resulting organic phase was dried under vacuum at room temperature for 12 h. To a solution of the obtained liquid (3 g) in dichloromethane (100 ml) was added a solution of $LiTf_2N$ (2g, 6.9 mmol) in water with stirring at room temperature. The solution was mixed at room temperature for 12 h, and the organic layer was separated and washed three times with water. The dichloromethane was removed by evaporation and the resulting liquid was dried under vacuum at 60 °C for 12 h. The resultant product was obtained as a colorless liquid.

$^1$H NMR (400 MHz, $CDCl_3$, $\delta$/ppm relative to TMS): 0.87 (t, $J$ = 14 Hz, 9H), 1.24-1.33 (m, 24H), 1.41-1.59 (m. 12H), 2.09-2.18 (m, 6H), 2.27-2.40 (m, 2H), 3.21 (s, 1H), 3.52-3.57 (m, 1H), 3.65-3.72 (m. 2H), 4.08 (s, 1H)

**4-(Tri-*n*-octylphosphonio)butanesulphonate(1)**

4-(Tri-*n*-octylphosphonio)butanesulphonate (**1**) was synthesized and purified according to the procedure described chapter 2.

Compound **5**(M, $n$ = 8) was prepared by slow evaporation of the methanol solution of **1** and $MTf_2N$, and the obtained mixture was further dried at 60 °C under vacuum for 24 h. The resultant product was obtained as viscous liquid.

**4-(Tri-*n*-hexylphosphonio)butanesulphonate**

Titled compound was prepared using same procedure described for 4-(tri-*n*-octylphosphonio)-butanesulphonate.

$^1$H NMR (400 MHz, $CDCl_3$, $\delta$/ppm relative to TMS): 0.89 (t, $J$ = 6.9 Hz, 9H), 1.31 (m, 12H), 1.49 (m, broad, 12H), 1.76 (m, 2H), 2.00 (m, 2H), 2.22 (m, 6H), 2.46 (m, 2H), 2.86 (t, $J$ = 7.3 Hz, 2H). ESI–TOF–MS: Calculated for $C_{22}H_{47}O_3PS$ $[M + Na]^+$ : m/z = 445.64; Found: 446.24. Elemental analysis: Calculated for $C_{22}H_{47}O_3PS$: C, 62.52; H, 11.21; O, 11.36; P, 7.33; S, 7.59. Found: C, 61.75; H, 11.52; N, 0%.

Compound **5**(*6*) was prepared by slow evaporation of the methanol solution of 4-(tri-n-hexylphosphonio)butanesulphonate and $LiTf_2N$, and the obtained mixture was further dried at 60 °C under vacuum for 24 h. The resultant product was obtained as viscous liquid.

**4-(Tri-*n*-octylphosphonio)pentanoic-acetate**

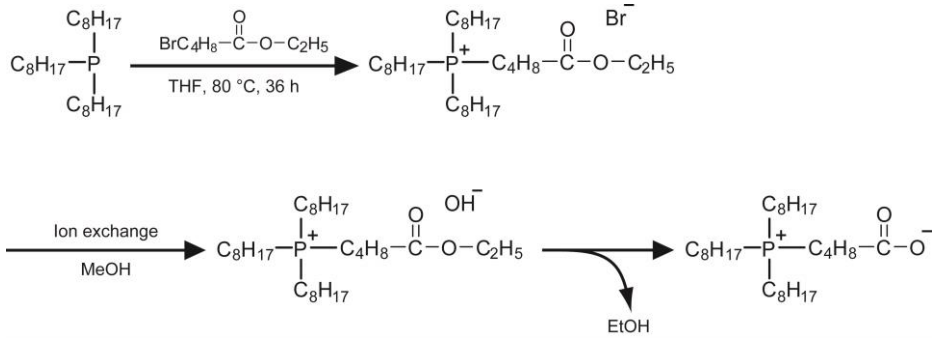


To a solution of tri-*n*-octylphosphine (8 g, 21.6 mmol) in THF was added a solution of ethyl 5-bromovalerate (5 g, 23.9 mmol) in THF with stirring at room temperature. The solution was heated as stirred at 80 °C for 36 h. After THF was evaporated, the product was purified with hexane three times. The obtained product dissolved in methanol and the resultant solution was passed through a column filled with anion exchange resin (Amberlite IRN-78). After stirring the resulting solution at room temperature for 48 h, methanol was removed by evaporation. The crude compounds were further purified by the recrystallization from ethylacetate. The ethylacetate was removed by evaporation and the resulting powder was dried under vacuum at room temperature for 12 h. The resultant product was obtained as a white powder.

$^1$H NMR (400 MHz, $CDCl_3$, $\delta$/ppm relative to TMS): 0.86 (t, $J$ = 13.6 Hz, 9H), 1.23-1.31 (m, 24H), 1.41-1.52 (m, 12H), 1.59-1.69 (m, 2H), 1.73-1.80 (m, 2H), 2.15-2.25 (m, 8H), 2.35-2.43 (m, 2H).

Compound **6** was prepared by slow evaporation of the methanol solution of 4-(tri-*n*-hexylphosphonio)butanesulphonate and $LiTf_2N$, and the obtained mixture was further dried at 60 °C under vacuum for 24 h. The resultant product was obtained as viscous liquid.

**2-(Tri-*n*-octylphosphonium)ethyl-ethylphosphoate**

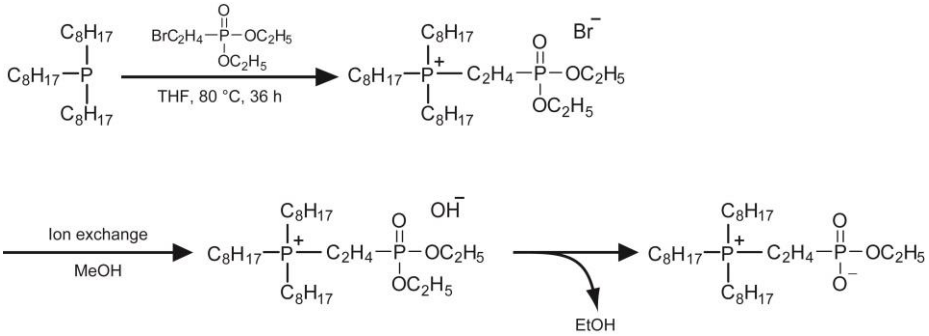


2-(Tri-*n*-octylphosphonium)ethyl-ethylphosphoate was synthesized as reported previously.[13] To a solution of tri-*n*-octylphosphine (5 g, 13.5 mmol) in THF was added a solution of diethyl-2-bromoethylphosphonate (3.3 g, 13.5 mmol) in THF with stirring at room temperature. The solution was heated as stirred at 80 °C for 36 h. After THF was evaporated, the product was purified with hexane three times. The obtained product dissolved in methanol and the resultant solution was passed through a column filled with anion exchange resin (Amberlite IRN-78) to give a hydroxide solution. After stirring the resulting solution at room temperature for 48 h, methanol was removed by evaporation. The crude compounds were further purified by the recrystallization from hexane. The hexane was removed by evaporation and the resulting powder was dried under vacuum at room temperature for 12 h. The resultant product was obtained as a white powder.

$^1$H NMR (400 MHz, $CDCl_3$, $\delta$/ppm relative to TMS): 0.87 (t, $J$ = 13.6 Hz, 9H), 1.22-1.32 (m, 27H), 1.42-1.56 (m, 12H), 1.72-1.84 (m, 2H), 2.24-2.31 (m, 6H), 2.40-2.5 (m, 2H), 3.92-3.99 (m, 2H).

Compound **7** was prepared by slow evaporation of the methanol solution of 2-(Tri-*n*-octylphosphonium)ethyl-ethylphosphoate and $LiTf_2N$, and the obtained mixture was further dried at 60 °C under vacuum for 24 h. The resultant product was obtained as viscous liquid.

**Tris(2-hydroxylethyl)methylammonium bis(trifluoromethanesulfonyl)imide (8)**

A solution of tris(2-hydroxyethyl)methylammonium methylsulfate (12 g, 43.6 mmol) in water (200ml) was passed through a column filled with anion exchange resin (Amberlite IRN-78) to give a solution of tris(2-hydroxyethyl)methylammonium hydroxide. To the resultant solution was dropwise added a solution of bis(trifluoromethanesulfonyl)imidic acid (13.5 g, 47.9 mmol) in water (20 ml) over a period of 30 min, and the resulting solution was stirred for 2 h at room temperature. The reaction mixture was evaporated under reduced pressure. The crude material was dissolved in acetone (100 ml) and then passed through a short column filled with active alumina (20 ml). The acetone was removed by evaporation and the resulting liquid was dried under vacuum at room temperature for 12 h. The resultant product was obtained as a colorless liquid.

$^1$H NMR (400 MHz, DMSO, $\delta$/ppm relative to TMS): 3.15 (s, 3H), 3.53 (t, $J$ = 10.6 Hz, 6H), 3.85 (s, 6H), 5.24 (s, 3H). Elemental analysis: calculated for $C_9H_{18}F_6N_2O_7S_2$: C, 24.33; H, 4.08; F, 25.65; N, 6.30; O, 25.20; S, 14.43. Found: C, 23.94; H, 3.88; N; 6.40%.

**Choline bis(trifuoromethylsulfonyl)imide (9)**

To a solution of choline bromide (5.0 g, 8.9 mmol) in dichloromethane (100 ml) was added a solution of $LiTf_2N$ (2.8 g, 9.8 mmol) in water with stirring at room temperature. The solution was mixed at room temperature for 12 h, and the organic layer was separated and washed three times with water. The dichloromethane was removed by evaporation and the resulting liquid was dried under vacuum at 60 °C for 12 h. The resultant product was obtained as a colorless liquid.

$^1$H NMR (400 MHz, DMSO, $\delta$/ppm relative to TMS): 3.07 (s, 9H), 3.36 (t, $J$ = 16.0 Hz, 2H), 3.77-3.82 (m, 2H), 5.24 (t, $J$ = 9.6Hz, 2H)

**1-(2-hydroxyethyl)-3-methylimidazolium bis(trifuoromethylsulfonyl)imide (10)**

To a solution of 1-methylimidazole in toluene was added a solution of 2-bromoethanol in toluene with stirring at room temperature. The solution was heated at 70 °C for 24 h. After toluene was evaporated, the crude material was further purified by recrystallization from ethylacetate /methanol 2/1 (v/v) solution, to give as a white powder. Then Br anion replaced with [$Tf_2N$] anion, using same procedure described for **3** but smaller amount of water was used for washing procedure.

$^1$H-NMR (400MHz, DMSO-$d_6$, $\delta$/ppm relative to TMS: 3.73 (q, $J$ = 5.3 Hz, 2H), 3.87 (s, 3H), 4.21 (t, $J$ = 4.0 Hz, 2H), 5.17 (t, $J$ = 6.00 Hz, 1H), 7.68 and 7.72 (w, $J$ = 2.00 and 2.00 Hz, 2H), 9.07 (s, 1H).

## Measurement

The thermal property of the materials were examined by differential scanning calorimetry (DSC, DSC6220, Seiko Instruments) from −100 to 250 °C at a heating/cooling rate of 10 °C/min. An Olympus BX51 optical polarizing microscope equipped with a Lincam hot-stage was used to examine thermal phase behavior of the materials. Wide-angle X-ray diffraction (WAXD) patterns were obtained using a Rigaku RINT-2500 diffractometer with Cu Kα radiation. The ionic conductivity was measured with an impedance analyzer (Schlumberger, Solartron 1260) using a Programmable Temperature Controller TXN-700; the heating rate was 2 °C/min. The comb-shaped gold electrodes were used to measure ionic conductivity parallel to the substrate.

## 3-5 References


1. D. Demus, J. W. Goodby, G. W. Gray, H. W. Spiess and V. Vill, *Handbook of Liquid Crystals*, Wiley-VCM, Weinheim, 1998.
2. C. Tschierske, Chem. *Soc. Rev.*, 2007, **36**, 1930.
3. S. Ueda, J. Kagimoto, T. Ichikawa, T. Kato and H. Ohno, *Adv. Mater.*, 2011, **23**, 3071.
4. (*a*) M. Yoshizawa, H. Hirao, K. Ito-Akita and H. Ohno, *J. Mater. Chem.*, 2001, **11**, 1057; (b) H. Ohno, M. Yoshizawa and W. Ogihara, *Electrochim. Acta*, 2003, **45**, 2079.
5. A. Arce, M. J. Earle, S. P. Katdare, H. Rodríguez and K. R. Seddon, *Chem. Commun*., 2006, 2548.
6. J. Kagimoto, S. Taguchi, K. Fukumoto and H. Ohno, *J. Mol. Liq.*, 2010, **153**, 133.
7. S. Bose, C. A. Barnes and J. W. Petrich, *Biotechnolo. Bioeng*., 109, **2**, 434.
8. (*a*) V. S. K. Balagurusamy, G. Unger, V. Percec and G. Johansson, *J. Am. Chem. Soc.*, 1997, **119**, 1539; (*b*) D. J. P. Yeardly, G. Ungar, V. Percec, M. N. Holerca and G. Johansson, *J. Am. Chem. Soc.*, 2000, **122**, 1684; (*c*) C. Tschierske, *J. Mater. Chem.*, 2001, **11**, 2647.
9. (*a*) J. N. Israelachivili, *Intermolecular and Surface Forces*, Academic Press, New York, 1985; (*b*) T. L. Greaves and C. J. Drummond, *Chem. Soc. Rev.*, 2008, **37**, 1709; (*c*) C. Tschierske, *Curr. Opin. Colloid Interface Sci*., 2002, **7**, 35.
10. (*a*) F. S. Bates and G. H. Fredrickson, *Annu. Rev. Phys. Chem.*, 1990, **41**, 525; (*b*) W. Chen and B. Wunderlich, Macromol. *Chem. Phys.*, 1999, **200**, 283.
11. (*a*) M. Yoshio, T. Mukai, H. Ohno and T. Kato, *J. Am. Chem. Soc.*, 2004, **126**, 994; (*b*) H. Shimura, M. Yoshio, K. Hoshino, T. Mukai, H. Ohno and T. Kato, *J. Am. Chem. Soc*., 2008, **130**, 1759.
12. F. Bellina, C. Chiappe and M. Lessi, *Green Chem.*, 2012, **14**, 148.
13. Y. Fukaya and H. Ohno, *Phys. Chem. Chem. Phys.*, 2013, **15**, 14941-14944.

# Chapter 4

## Evaluation of nano-segregated ionic liquid systems

# 4-1 Introduction

Recently, there have been increasing attention to the strategy to mix two or more ILs because this strategy provides novel IL systems that are unattainable by a single ion pair.[1] In chapter 3, the author reported a novel binary IL system forming nano-segregated LC structures by suitably designing hydrophobic phosphonium-type ILs and a hydrophilic ammonium-type IL. The formation of the nano-segregated LC structures is attributed to the incompatibility between the hydrophobic phosphonium cation and the hydrophilic ammonium cation. The author has expected that these nano-segregated IL systems may act as a nano-biphasic IL system where two immiscible IL nano-domains coexist homogeneously in a macroscopic scale, and then affords an IL matrix showing properties and functions derived from both two IL nano-domains.

The author's aim here is to clarify if there are two immiscible IL nano-domains in the nano-segregated IL system. The author considers that to prove the presence of two independent IL nano-domains with different polarities in the system is the best way for the verification of the construction of nano-biphasic IL systems. For evaluating polarity in nano-segregated IL domains, the author has focused on the use of solvatochromic probes because, in the case of normal ILs, the evaluation of polarity by solvatochromic probes is a frequently-used method[2,3] and moreover this method is useful for evaluating physicochemical properties, such as polarity[4] and viscosity[5], in local environment.

In this chapter, first, the author has carefully selected suitable solvatochromic dyes dissolving selectively in either hydrophilic or hydrophobic ILs. Then, the author has evaluated the local polarity in the nano-segregated IL systems by examining UV-vis absorption property of these dyes. In addition, the author evaluated local viscosity of each nano-segregated IL domain by using fluorescence anisotropy measurement.

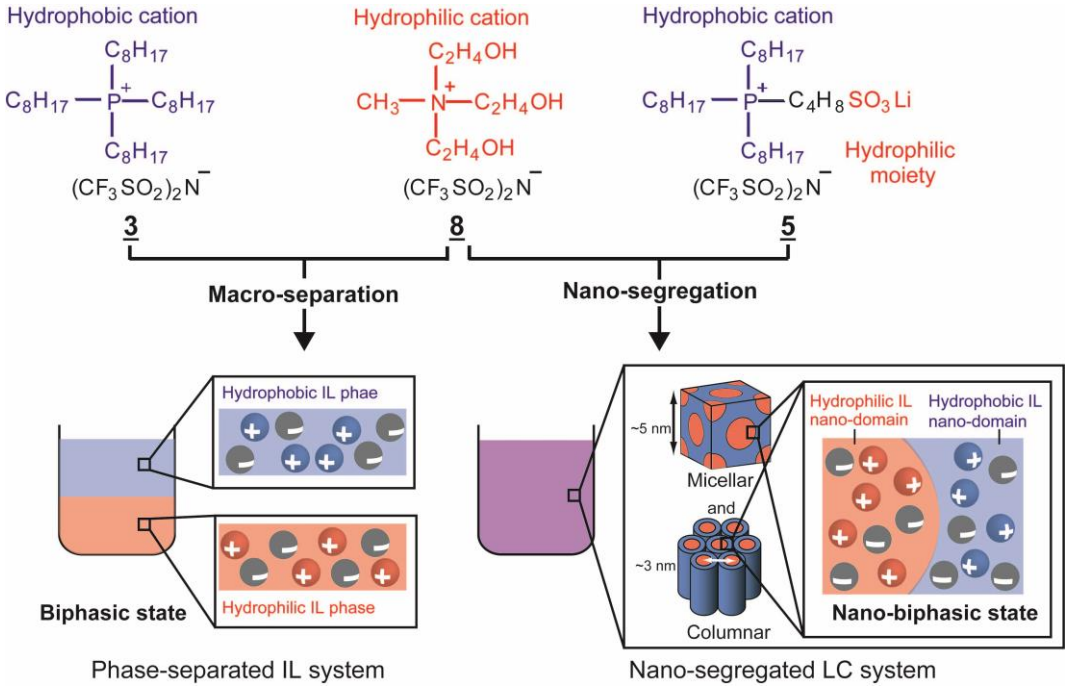


**Figure 4-1** Structure of hydrophobic phosphonium-type IL (**3**), hydrophilic ammonium-type IL (**8**) and phosphonium-type IL having a hydrophilic ion pair at the periphery of an alkyl chain (**5**). The mixture of **3** and **8** forms a macro-separated IL system. The combination of **5** and **8** provides nano-segregated IL systems forming micellar and columnar structures

# 4-2 Results and discussion

## 4-2-1 Preparation of a macro-separated ionic liquids system

To find solvatochromic dyes dissolving selectively in either hydrophobic or hydrophilic ILs, the author prepared a macro-separated IL system and then examined partition behavior of various dyes in it. The macro-separated IL system was designed to consist of hydrophilic and hydrophobic phases by using hydrophobic phosphonium-type IL **3** containing long alkyl chains on the cation and hydrophilic ammonium-type IL **8** containing multiple hydroxyl groups on the cation (Fig. 3-1, left). An equal-weight mixture of **3** and **8** forms a stable macroscopic phase separation where the upper phase is mainly composed of **3** (hydrophobic IL phase) and the lower phase is mainly composed of **8** (hydrophilic IL phase). The macro-phase separation of these two ILs is attributed to the incompatibility of the hydrophobic phosphonium cation and the hydrophilic ammonium cation. It has been reported that the density of ILs having phosphonium cations is lower than that of ILs having other cations.[6] Below, the author describes the exploration of dyes possessing two abilities: one is to dissolve selectively in either hydrophilic or hydrophobic ILs, and the other is to show solvatochromic behavior in various solvents including ILs.

## 4-2-2 Selection of solvatochromic dyes dissolving selectively in either hydrophobic or hydrophilic ILs

### Partition behavior of various dyes in the macro-separated IL system

As a preliminary experiment, the author examined the partition of dyes in the macro-separated IL system. Various dyes were added to the macro-separated IL system composed of **3** and **8** at room temperature (Figure 4-2). Among a number of dyes, it was found that Sudan IV, 4-(4-butylphenylazo)phenol and 3,4'-dihexyl-2,2'-bithiophene (BTP), high-selectively dissolved in the hydrophobic IL phase. The partition behavior of BTP in the macro-separated IL system was examined by the UV-vis absorption measurement because this dye has little absorption in the visible region. The selective dissolution of these dyes in the hydrophobic IL phase can be explained by their hydrophobic molecular structures. In contrast, dyes having multiple ionic groups, such as naphthol yellow S (NYS) and CBB G-250, selectively dissolved in the hydrophilic IL phase. These results are comprehensible to be due to high compatibility between the hydroxyl groups on the tris(2-hydroxyethyl)-ethylammonium cation of **8** and the ionic moiety of these dyes. Other dyes, such as 5-bromo-5"-formyl-2,3":5',2"-terthiophene, Nile red, rhodamine 6G, rhodamine B, coumarine 153, indoine blue and indigo, did not show highly selective dissolution in each IL phase.

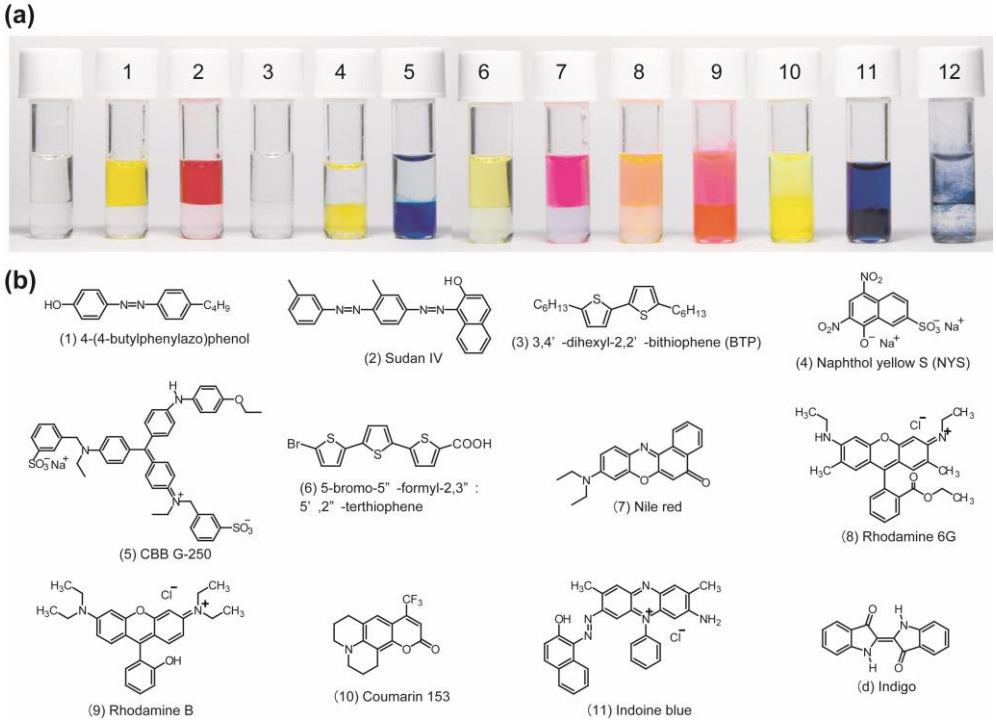


**Figure 4-2** (a) Partition behavior of various dyes such as (1) 4-(4-butylphenylazo) phenol, (2) Sudan IV, (3) 3,4'-dihexyl-2,2'-bithiophene, (4) naphthol yellow S, (5) CBB G-250 (6) 5-bromo-5"-formyl- ,3":5',2" -terthiophene, (7) Nile red, (8) rhodamine 6G, (9) rhodamine B, (10) coumarine 153, (11) indoine blue and (12) indigo in the macro-separated IL system composed of **3** and **8**. (b) Structure of these dyes used in the partition experiments.

Evaluation of solvatochromic behavior in molecular solvents and ionic liquids

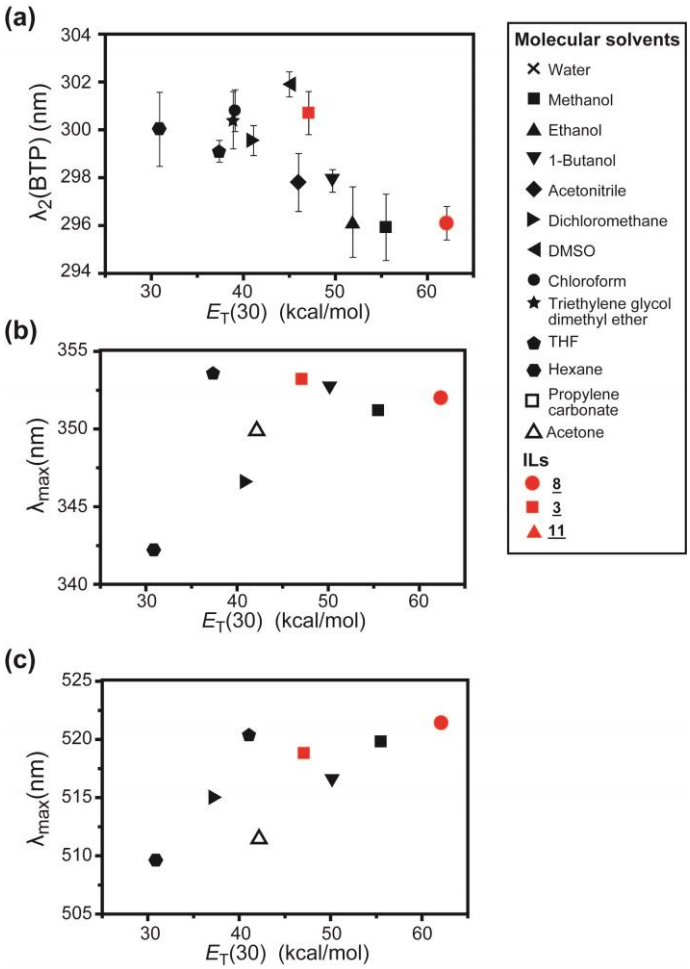


**Figure 4-3** Comparison of the value of $E_T(30)$ in some conventional molecular solvents and ILs and the absorbance peak of (a) BTP ($\lambda_2$(BTP)), (b) 4-(4-butylphenylazo)phenol ($\lambda_{max}$) and (c) Sudan IV ($\lambda_{max}$). $E_T(30)$ values of conventional solvents are taken from ref. 7 and 8.

For these three dyes showing highly selective dissolution in the hydrophobic IL phase, the author examined the solvatochromic behavior in some conventional molecular solvents having various polarity parameter $E_T(30)$. The $E_T(30)$ is a parameter that is calculated from the molar electron transition energy of Reichardt's dye 30 in the solvents, which is the most common measure of polarity. Recently, this parameter has been successfully employed, not only for molecular solvents[7] but also for ILs.[2]

To evaluate solvatochromic behaviour of BTP, the author performed UV-vis absorption measurements in various solvents. BTP showed two absorbance peaks at around 250 nm ($\lambda_1$(BTP)) and 300 nm ($\lambda_2$ (BTP)). In this study, the author focused on $\lambda_2$(BTP) for evaluating the polarity in ILs because some ILs, including IL **8**, have absorption at around 250 nm. Figure 4-3a shows the relationship between the peak wavelengths of $\lambda_2$(BTP) in some conventional solvents and their

$E_T(30)$. The absorption peaks of BTP in various molecular solvents are negatively correlated with the value of $E_T(30)$. For example, the $\lambda_2$(BTP) is observed at 296 nm in methanol having high $E_T(30)$ = 51.9 kcal/mol while the $\lambda_2$ (BTP) in hexane with low $E_T(30)$ = 39.1 kcal/mol is observed at 300 nm. It should be pointed out that negative solvatochromism is observed also in ILs. These results lead us to consider that BTP is a suitable dye for evaluating the polarity in hydrophobic nano-domains.

On the other hand, the absorption peaks of Sudan IV and 4-(4-butylphenylazo)phenol in various molecular solvents and ILs are positively correlated with the value of $E_T(30)$ (Figure 4-3b and 4-3c). However, the difference in the absorption peak wavelength of Sudan IV in **3** and **8** is small, despite the difference in the value of $E_T(30)$ of each IL is significantly large. Moreover, the relationship between the absorption peaks of 4-(4-butylphenylazo)phenol in ILs (**3** and **8**) and the value of $E_T(30)$ of each IL does not follow a trend of the correlation of the absorption peaks of the dye in molecular solvents with the value of $E_T(30)$. Considering these results, the author determined that Sudan IV or 4-(4-butylphenylazo)phenol are not suitable for evaluating the polarity in ILs.

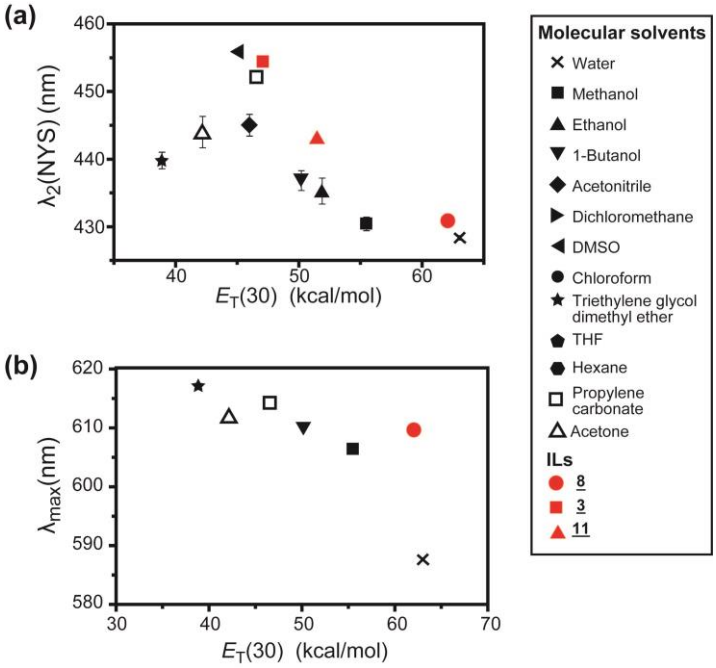


**Figure 4-4** Comparison of the value of $E_T(30)$ in some conventional molecular solvents and ILs and the absorbance peak of (a) NYS ($\lambda_2$(NYS)) and (b) CBB G-250 ($\lambda_{max}$). $E_T(30)$ values of conventional solvents are taken from ref. 7 and 8.

The author examined the solvatochromic behavior of NYS and CBB G-250 that dissolve selectively in the hydrophilic IL phase in various molecular solvents and ILs. There are two peaks in the UV-vis spectra of NYS. One is observed at around 390 nm ($\lambda_1$(NYS)) and the other is observed at around 440 nm ($\lambda_2$(NYS)). In this study, the author focused on the wavelength change of $\lambda_2$(NYS) because it has been reported that this peak significantly shifts depending on the external environment.[9] The absorption peaks of NYS in various molecular solvents are negatively correlated with the value of $E_T$(30) (Figure 4-4a). For example, the $\lambda_2$(NYS) is observed at 429 nm in water ($E_T$(30) = 63.1 kcal/mol), whereas the $\lambda_2$(NYS) is observed at 451 nm in propylene carbonate ($E_T$(30) = 39.1 kcal/mol). It is of importance that NYS also showed negative solvatochromism behavior even in ILs. On the other hand, the absorption peak of CBB G-250 in solvents exhibited negative correlation with the value $E_T$(30) (Figure 4-4b). However, the solvatochromic behavior of CBB G-250 in ILs is not clear because its solubility in **3** is below the detection limits. These results lead us to consider that NYS is a suitable dye for evaluating the polarity in hydrophilic nano-domains. Through all results above mentioned, the author decided to use BTP and NYS for evaluating the polarity in the nano-segregated IL systems.

## 4-2-3 Polarity evaluation for the nano-segregated ionic liquid systems

For the evaluation of polarity in the nano-segregated IL systems, the author measured UV-vis absorption of BTP and NYS in **5**/**8** mixtures. It was found that BTP shows two absorbance peaks in **5**/**8** mixtures as well as in conventional solvents. For example, the UV-vis spectrum of BTP in **5**/**8** mixture (mole fraction 0.35 for **8**) shows $\lambda_1$(BTP) at 251 nm and $\lambda_2$(BTP) at 301 nm (Figure 4-5). Focusing on the $\lambda_2$(BTP) value, it is assumed that the polarity in **5**/**8** mixtures is low comparable to those of conventional solvents with $E_T$(30) ranging from 30 to 45 kcal/mol. On the other hand, NYS shows two absorbance peaks in **5**/**8** mixtures as well as in conventional solvents. For example, the UV-vis spectrum of NYS of **5**/**8** mixture (mole fraction 0.35 for **8**) shows $\lambda_1$(NYS) at 387 nm and $\lambda_2$(NYS) at 424 nm (Figure 4-5). Focusing on the $\lambda_2$(NYS) value, it is assumed that the polarity in **5**/**8** mixture (mole fraction 0.35 for **8**) is high comparable to those of conventional solvents with $E_T$(30) ranging 60 to 65 kcal/mol. These absorption peaks are observed at almost the same position independent of the composition ratio of **5** and **8**. For example, the $\lambda_2$(NYS) value in **5**/**8** mixture (mole fraction 0.50 for **8**) forming the columnar structure is 423 nm, which is comparable to that of in **5**/**8** mixture (mole fraction 0.35 for **8**) forming a micellar cubic structure (Table 4-1). As well as $\lambda_2$(NYS), $\lambda_2$(BTP) also shows little peak position change. These results suggest that the composition ratio of **5** and **8** scarcely influence the polarity in the mixtures while it changes the dimensional order of the nano-segregated structures.

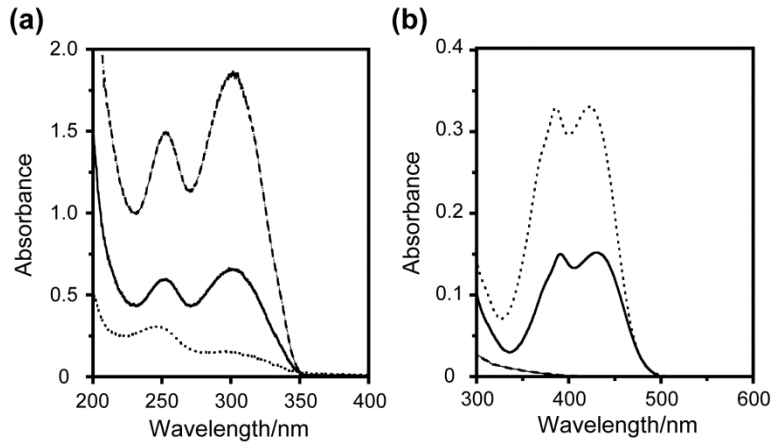


**Figure 4-5** UV-vis absorption spectra of (a) BTP and (b) NYS in the hydrophobic IL phase (dashed line), the hydrophilic IL phase (dotted line) and the nano-segregated IL system formed by **5**/**8** mixture (mole fraction 0.35 for **8**), (black line).

**Table 4-1** UV-vis absorption wavelength of BTP and NYS in ILs, the macro-separated IL system and the nano-segregated IL system[a]

| Solvent | $\lambda_2$(BTP) (nm) | $\lambda_2$(NYS) (nm) |
|---|---|---|
| Hydrophobic IL **3** | 300 | 454 |
| Hydrophilic IL **8** | 297 | 431 |
| Hydrophobic IL phase | 295 | 429 |
| Hydrophilic IL phase | 302 | — |
| **5**/**8** mixture (mole fraction 0.35 for **8**) | 301 | 424 |
| **5**/**8** mixture (mole fraction 0.50 for **8**) | 303 | 423 |

[a] Measured at room temperature. —not detected.

Based on the above results, the author discusses the polarity in the nano-segregated IL system. Although the solvatochromic behavior of BTP in **5**/**8** mixtures indicates that **5**/**8** mixtures are less polar solvents with $E_T(30)$ ranging from 30 to 45 kcal/mol, that of NYS indicates **5**/**8** mixtures are polar solvents with $E_T(30)$ ranging from 60 to 65 kcal/mol. For the explanation of these inconsistent results, it is required to assume that **5**/**8** mixtures have two domains with different polarities and these dyes are partitioned to each domain. Considering two results: one is that NYS prefers to dissolve in hydrophilic solvents while BTP prefers to dissolve in hydrophobic solvents in the macro-separated IL system, and the other is that the nano-segregated IL system forms micellar cubic or columnar structures consisting of hydrophilic inner nano-domain and hydrophobic outer nano-domain, it is reasonable to assume that NYS and BTP are severally partitioned to the each nano-domain in the nano-segregated IL system, thus giving the local polarity in the inner and outer

domains, respectively. Moreover, the $\lambda_2$(BTP) in **5**/**8** mixtures are observed at almost the same position as that observed in **3** (300 nm), suggesting that the hydrophobic outer domain of **5**/**8** mixtures have **3** like environment. On the other hand, the $\lambda_2$(NYS) value in **5**/**8** mixtures (424 and 423 nm) is comparable to or smaller than that of in **8** (431 nm), which suggests that **5**/**8** mixtures form a hydrophilic inner nano-domains whose polarity is comparable to or slightly higher than that of **8**. Considering these results, it is reasonable to assume that the nano-segregated IL systems provide a novel IL matrix where two distinct IL domains coexist with keeping their original polarities, which deserves to be called a nano-biphasic IL system. The author should note here that there is a possibility that the polarity of the inner nano-domains increased by the formation of curved interface. A unique characteristic in the nano-biphasic IL system is that it has huge interface area between the hydrophobic and the hydrophilic IL domains. According to the rough calculation, the area of hydrophobic/hydrophilic interface in the nano-biphasic system is approximately $10^6$ times larger than that in the macro-separated IL system. The author envisions that this huge interface area between hydrophobic and hydrophilic IL domains has potential to be used for novel separation and reaction fields.

## 4-2-4 Local viscosity evaluation for the nano-segregated ionic liquid systems

Fluorescence dyes also can be used as probes to evaluate their surrounding environment.[3c] Fluorescence anisotropy measurement reveals the average angular displacement of the fluorescence dye that is dependent upon the rate and extent of rotational diffusion.[11] The rotational diffusion depends on the viscosity of the solvent and the size and shape of the rotating molecules. Therefore, the local viscosity of micelle[12] and block polymer[5] was estimated by using fluorescence anisotropy. In this section, the author has evaluated the local viscosity in the nano-segregated IL systems by examining fluorescent anisotropy of fluorescence dyes dissolving selectively in either hydrophilic or hydrophobic ILs.

### Selection of fluorescent dyes dissolving selectively in either hydrophobic or hydrophilic ILs

To measure the local viscosity in the nano-segregated IL systems, first, the author has examined the partition of fluorescent dyes in the macro-separated IL system (Figure 4-6). Through the partition measurement of various dyes, the author found that 1,6-diphenyl-1,3,5-hexatriene (DPH) is selectively dissolved in the hydrophobic IL phase. On the other hand, sulforhodamine B (SRB) shows selective dissolution in the hydrophilic IL phase. As showed in section 4-2-2, these results are

able to be explained by the compatibility between dyes and ILs.

The author observed the fluorescence of DTP and SRB in the macro-separated IL system and the nano-segregated IL system. The results are presented in Figure 4-7. It was found that DPH shows three emission peaks in **5**/**8** mixtures as well as in conventional solvents. For example, the fluorescent spectrum of DPH in **5**/**8** mixture (mole fraction 0.35 for **8**) shows three peaks at 406 nm, 428 nm and 451 nm (Figure 4-7a). On the other hand, SRB shows an emission peak as well as in conventional solvents. For example, the fluorescent spectrum of DPH in **5**/**8** mixture (mole fraction 0.35 for **8**) shows a peak at 579 nm (Figure 4-7b).Considering these results above mentioned in this section, the author decided to use DPH and SRB for evaluating the viscosity in the nano-segregated IL systems.

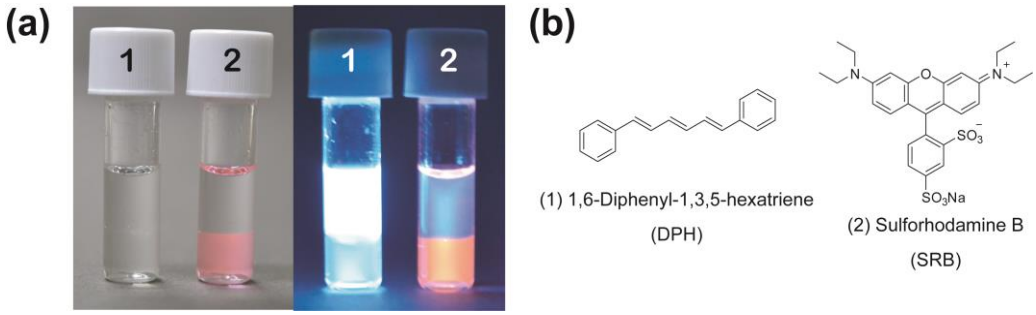


**Figure 4-6** (a) Partition behavior of (1) 1,6-diphenyl-1,3,5-hexatriene (DPH) and (2) sulforhodamine B (SRB). The picture on the left was taken in daylight and the picture on the right was taken under UV illumination (365 nm). (b) Structure of dyes used in the partition experiment.

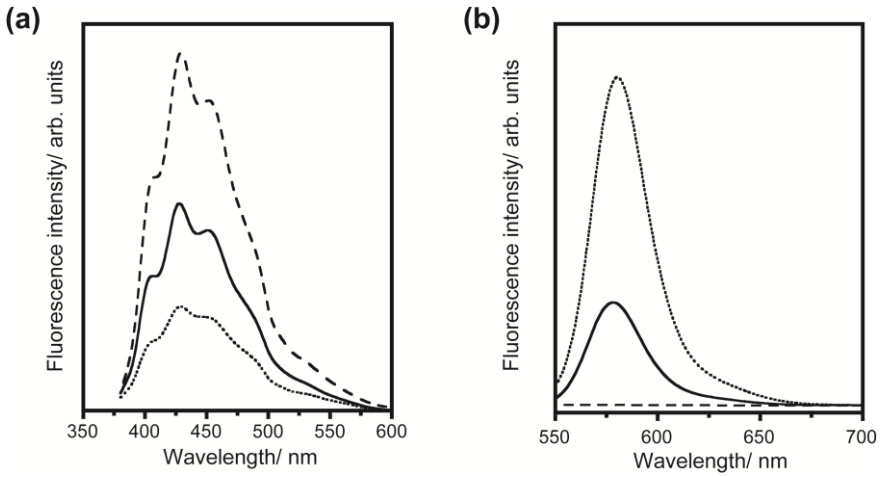


**Figure 4-7** Florescence spectra of (a) DPH and (b) SRB in the hydrophobic IL phase (dashed line), the hydrophilic IL phase (dotted line) and the nano-segregated IL system formed by **5**/**8** mixture (mole fraction 0.35 for **8**), (black line).

## Evaluation of fluorescent anisotropy in the nano-segregated ionic liquid systems

To evaluate local viscosity in the hydrophobic outer domain of nano-segregated IL system, the author measured fluorescent anisotropy of DPH in **5**/**8** mixtures at various temperature (Figure 4-8a). It can be seen that the anisotropy of DPH in **5**/**8** mixtures gradually decreases with the increase of the temperature (Figure 4-8a). Decrease of the anisotropy is due to the increase of the rotational diffusion rate of DPH. The rotational diffusion rate is depending on the local viscosity. It is assume that the local viscosity is decreased with the increase of temperature. It is noteworthy that the anisotropy of DPH in **5**/**8** mixture (mole fraction 0.35 for **8**, ●) increase drastically at around 100 ºC. The author has reported that **5**/**8** mixture (mole fraction 0.35 for **8**) shows phase transition from micellar cubic phase to isotropic state at 96 ºC. Considering these, it is reasonable to assume that the increase of anisotropy is due to the phase transition behavior of **5**/**8** mixture (mole fraction 0.35 for **8**) and the viscosity of hydrophobic domain in the nano-segregated system is lower than that of isotropic state. In contrast, the anisotropy value drastically change of DPH was not observed in **5**/**8** mixture (mole fraction 0.50 for **8**, □), while the sample shows phase transition from columnar to isotropic at 25 ºC. **5**/**8** mixture (mole fraction 0.00 for **8**, ○) forms a cubic structure −12 to 196 ºC shows gradually decreases of the anisotropy value with the increase of the temperature.

For the evaluation of local viscosity in the hydrophilic inner domain of nano-segregated IL systems, the author performed anisotropy measurement of SRB in **5**/**8** mixtures (Figure 4-8b). As well as anisotropy of DPH in **5**/**8** mixture (mole fraction 0.35 for **8**), the drastically increase of anisotropy of SRB in **5**/**8** mixture (mole fraction 0.35 for **8**) is also observed at around 100 ºC. This result also suggested that the viscosity of a cubic phase is lower than that of the isotropic state. The anisotropies of SRB in **5**/**8** mixture (mole fractions 0.00 and 0.35) forming nano-segregated structures show slightly value change with the increase of the temperature. These results show that the viscosity in the nano-segregated systems is relatively insulated from the influence of the temperature. The anisotropy values of SRB in **5**/**8** mixtures are comparable to or higher those in **8**, which suggest that **5**/**8** mixtures forms a hydrophilic inner nano-domains whose viscosity is comparable to or slightly higher than that of **8**.

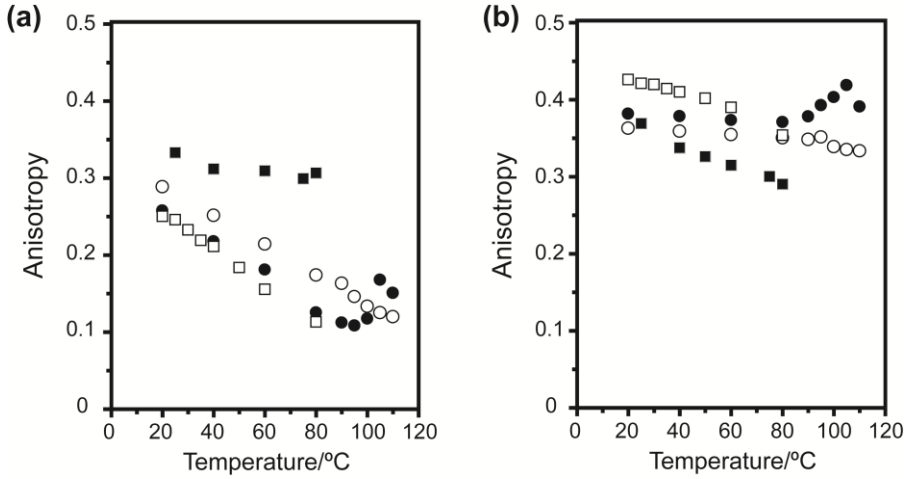


**Figure 4-8** Temperature-dependent fluorescent anisotropy of (a) DPH and (b) SRB in **5**/**8** mixtures (mole fraction X for **8**). X = 0 (○), 0.35 (●), 0.50 (□) and 1.00 (■).

It is value to estimate the local viscosity in nano-segregated IL systems. The Perrin equation[13] (4-1) gives a simple relation between the anisotropy (r) and the viscosity ($\eta$)

$$\frac{1}{r} = \frac{1}{r_0} + \frac{kT\tau}{\eta V r_0} \quad (4\text{-}1)$$

where $r_0$ is anisotropy at t = 0, $\tau$ is the average lifetime of the fluoroprobe emission, $k$ is the Boltzmann constant and $V$ is the effective molecular volume. Eqn 4-1 predicts a linear relationship between $1/r$ and $T/\eta$. The author measured anisotropy and viscosity at various temperatures in glycerol and several ILs (Figure 4-9). It can be seen that slopes of each solvent are widely different. Eqn 4-1 indicate that $1/r$ is affected by not only $T$ and $\eta$ but also $V$ and $\tau$. In the course study, $\tau$ is very influenced by surrounding environment such as polarity. Considering this, it is assumed that the difference of the slope is due to the lifetime.

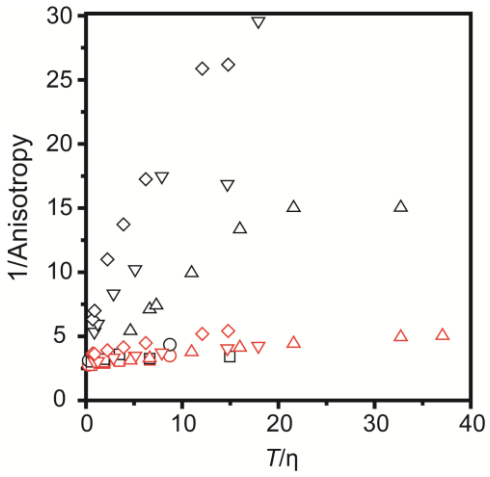


**Figure 4-9** Perrin plots of DPH (black) and SRB (red) in Glycerol and ionic liquids. Glycerol (○), **5** (□), **11** (△), **3** (◇) and **12** (▽).

## 4-3 Conclusions

The author has evaluated the local properties, such as viscosity and polarity, in a nano-segregated IL system. The nano-segregated IL system has been prepared by mixing a hydrophilic ammonium-type IL (**8**) and a hydrophobic phosphonium-type IL having a hydrophilic ion pair (**5**). For the polarity evaluation in the two nano-segregated domains, the author has carefully selected solvatochromic dyes that selectively dissolve in either hydrophilic or hydrophobic solvents. Through partition experiments in a macro-separated IL system consisting of hydrophilic and hydrophobic IL phases, it has been found that NYS and BTP are potential solvatochromic dyes. As well as in the macro-separated IL system, NYS and BTP are separately partitioned into the inner hydrophilic and outer hydrophobic domains, and then the solvatochromic behavior of these dyes gives an important insight that the polarity in the inner domain is comparable to that in hydrophilic ILs whereas that in the outer domain is comparable to that in hydrophobic ILs. These results suggest that the present nano-segregated mixture of ILs deserves to be called a nano-biphasic IL system.

For the evaluation of local viscosity, the fluorescent anisotropy of dyes in the nano-segregated IL systems were measured by using dyes selectively dissolve in either hydrophilic or hydrophobic ILs. By using partition experiment, the author decided to use DPH and SRB for evaluating the fluorescent anisotropy. The anisotropy measurements suggeste that the local viscosity of nano-segregate state is lower than that of isotropic state. In addition, the anisotropy value of inner hydrophilic domain is comparable to or little higher than that of the hydrophilic IL. These results suggested that the nano-segregated IL system has potential to be used as novel reaction fields. The author believes that the attempt to design nano-biphasic IL systems may be a strategy for developing new IL-based materials with innovative functions that are hard to produce by one-component IL system.

# 4-4 Experimental

## Materials

Sudan IV, 4-(4-butylphenylazo)phenol, naphthol yellow S, 5-bromo-5”-formyl -2,3”:5’,2”-terthiophene, rhodamine B, sulforhodamine B and tributyl-n-octylphosphonium bromide were purchased from Tokyo Chemical Industry, Co. Ltd. Indoine blue, coumarin 153 and 1,6-diphenyl-1,3,5-hexatriene were purchased from Sigma Aldrich. CBB G-250 and Nile red were purchased from Wako Chem. Co. Rhodamine 6G, indigo and 1-butyl-3-methylimidazolium bis(trifluoromethylsulfonyl)imide (**11**) were purchased from Kanto chemical co., Inc. Tributyl-*n*-octylphosphonium bromide was washed by hexane before use. All other commercially available chemicals were used as received.

## Synthesis of ILs

The characterization of these compounds was performed by $^1$H NMR (α-400, JEOL), ESI-MS and elemental analysis.

**Tributyl-*n*-octylphosphonium bis(trifluoromethylsulfonyl)imide (12)**

To a solution of tributyl-*n*-octylphosphonium bromide (5.0 g, 12.6 mmol) in dichloromethane (100 ml) was added a solution of lithium bis(trifluoromethylsulfonyl)imide ($LiTf_2N$) (4.0 g, 13.9 mmol) in water with stirring at room temperature. The solution was mixed at room temperature for 12 h, and the organic layer was separated and washed three times with water. The dichloromethane was removed by evaporation and the resulting liquid was dried under vacuum at 60 °C for 12 h. The resultant product was obtained as a colorless liquid.

$^1$H NMR (400 MHz, $CDCl_3$, $\delta$/ppm relative to TMS): 0.85 (t, $J$ = 14 Hz, 3H), 0.96 (t, $J$ = 14 Hz, 9H), 1.26-1.31 (m, 8), 1.47-1.52 (m, 16H), 2.06-2.14 (m, 8)

## General measurements

UV-vis absorption spectra were obtained with UV-2550 Shimadzu (resolution: 0.1 nm) at room temperature. Thermal property of the materials was examined by differential scanning calorimetry (DSC, DSC6220, Seiko Instruments) from −100 to 250 °C at a heating/cooling rate of 10 °C/min. An Olympus BX51 optical polarizing microscope equipped with a Lincam hot-stage was used to examine thermal phase behavior of the materials. Wide-angle X-ray diffraction (WAXD) pattern was obtained using a Rigaku RINT-2500 diffractometer with CuKα radiation. Two-dimensional small-angle X-ray scattering (2D SAXS) pattern was also recorded using an image plate detector (R-AXIS DS3C).

## Partition experiment of dyes in the macro-separated IL system

A macro-separated IL system was prepared by mixing **3** (1.0 g) and **8** (1.0 g). For partition experiments of various dyes in the macro-separated IL system, 0.5 mg of dyes were directly added. Mixture was first vigorously-stirred overnight, then left to settle until the separated phases become clear. The partition of dyes was confirmed by naked eye. The partition ratio was evaluated from the absorbance of dyes in each IL phase

## Sample preparation for UV-vis absorption measurements in the nano-segregated IL system

A stock solution of methanol or chloroform with dyes (1 mg $ml^{-1}$) was prepared. The stock solution (125 ml) was added to the methanol solutions of **5**/**8** mixture in various ratios. The total weight of **5**/**8** mixture is 0.5 g. The obtained solutions were dropped on an assembly cell (optical length: 0.1 mm) and dried on hotplate at 40 °C. The samples were exposed to under vacuum at room temperature for 1 h to remove methanol or chloroform.

## Solvatochromic probe analysis

Polarity parameter $E_T(30)$ was determined from the electronic transition energy of Reichardt's dye 33 ($E_T(33)$, eqn (4-2)) using following correlation, shown in eqn (4-3). Reichardt's dye 33 was used instead of Reichardt's dye 30 because it has been reported that Reichardt's dye 33 is more suitable for evaluating polarity in ILs.[10]

$$E_T(33) = hcN_A/\lambda(\text{Reichardt's dye 33})_{max} \quad (4\text{-}2)$$

$$E_T(30) = 0.9986E_T(33) - 8.6878 \quad (4\text{-}3)$$

## Fluorescence measurements

Fluorescence emission spectra of DPH and SRB in various solvent were measured with FP-8300 JASCO using 350 and 520 nm excitation wavelength, respectively. The fluorescence anisotropy was obtained by measuring the fluorescence intensities polarized parallel ($I_{\parallel}$) and perpendicular ($I_{\perp}$) to the direction of the polarized excitation. The emission intensities from DPH and SRB were detected at 430 and 580 nm, respectively. Degree of anisotropy is calculated by the following equation (4-4):

$$r = \frac{I_{\parallel} - GI_{\perp}}{I_{\parallel} + 2GI_{\perp}} \quad (4\text{-}4)$$

where $G$ is the correction factor.

## 4-5 References


1. H. Niedermeyer, J. P. Hallett, I. J. Villar-Garcia, P. A. Hunt and T. Welton, *Chem. Soc. Rev.*, 2012, **41**, 7780.
2. (*a*) C. Reichardt, *Green Chem.*, 2005, **7**, 339; (*b*) L. Crowhurst, P. R. Mawdsley, J. M. Perez-Arlandis, P. A. Salter and T. Welton, *Phys. Chem. Chem. Phys.*, 2003, **5**, 2790.
3. (*a*) S. N. V. K. Aki, J. F. Brennecke and A. Samanta, *Chem. Commun.*, 2001, 413; (*b*) A. J. Carmichael and K. R. Seddon, *J. Phys. Org. Chem.*, 2000, **13**, 591; (*c*) S. Pandey, S. N. Baker, S. Pandey and G. A. Baker, *J. Fluoresc.*, 2012, **22**, 1313.
4. C. D. Grant, M. R. DeRitter, K. E. Steege, T. A. Fadeeva and E. W. Castner, Jr, *Langmuir*, 2005, **21**, 1745.
5. (*a*) H. Shirota, Y. Tamoto and H. Segawa, *J. Phys. Chem. A*, 2004, **108**, 3244; (*b*) C. D. Grant, K. E. Steege, M. R. Bunagan and E. W. Castner, Jr, *J. Phys. Chem. B*, 2005, **109**, 22273; (*c*) B. Li, Y. Wang, X. Wang, S. Vdovic, Q. Guo and A. Xia, *J. Phys. Chem. B*, 2012, **116**, 13272.
6. (*a*) R. E. D. Sestro, C. Corley, A. Rebertson and J. S. Wilkes, *J. Organomet. Chem.*, 2005, **690**, 2536; (*b*) J. Kagimoto, S. Taguchi, K. Fukumoto and H. Ohno, *J. Mol. Liq.*, 2010, **153**, 133.
7. C. Reichardt, *Chem. Rev*., 1994, **94**, 2319.
8. M. J. Muldoon, C. M. Gordon and I. R. Dunkin, *J. Chem. Soc., Perkin Trans. 2*, 2001, **2**, 433.
9. J. Tas, P. Oud and J. James, *Histochemistry*, 1974, **40**, 231.
10. (*a*) C. P. Fredlake, M. J. Muldoon, S. N. V. K. Aki, T. Welton and J. F. Brennecke, *Phys. Chem. Chem. Phys.*, 2004, **6**, 3280; (*b*) B. R. Mellein, S. N. V. K. Aki, R. L. Ladewski and J. F. Brennecke, *J. Phys. Chem. B*, 2007, **111**, 131.
11. (*a*) J. R. Lakowicz, *Principles of fluorescence spectroscopy*, Springer (New York), 3rd edn, 2006; (*b*) F. M. Winnik and S. T. A. Regismond, *Colloids Surf. A*, 1996, **118**, 1.
12. K. Nakashima, T. Anzai and Y. Fujimoto, *Langmuir*, 1994, **10**, 658.
13. F. Rerrin, *Ann. Phys.* (Paris), 1929, **12**, 169.

# Chapter 5

## General Conclusions

This thesis details a new class of IL mixtures where two incompatible ILs coexist homogeneously in a macroscopic scale. ILs are an attractive material because their properties and functions can be tuned through the design of their cations and anions. One potential approach to functionalizing ILs is to mix two or more ILs. However, it is difficult to combine two incompatible ILs, such as hydrophobic and hydrophilic ILs, by simple IL mixing because their mixtures form macro-separation and/or ion exchange. In this thesis, the author proposed strategies to construct novel binary IL systems where two incompatible ILs coexist homogeneously in a macroscopic scale.

Chapter 1 introduced ILs and described IL mixtures. The objective of this thesis was also mentioned.

In chapter 2, a strategy to combine two immiscible ILs using a zwitterionization of a hydrophobic IL was proposed. A phosphonium-type zwitterion with long alkyl chains and a hydrophilic amino acid IL mixture is obtained as transparent gel. This mixture thermotropically forms a gel state via dispersed aggregation of the phosphonium-type zwitterion. These dispersed particles are produced by two competing effects: the aggregation of the phosphonium-type zwitterion through hydrophobic interactions, and the solvation of the phosphonium-type zwitterion by the amino acid IL via electrostatic interactions and hydrogen bonding. The activation energy of this gel-forming mixture is almost the same as that of the amino acid IL. This result indicates that the micro-segregation state can maintain their original mobility of the hydrophilic IL even after the addition of zwitterion. Increasing the mole fraction of the hydrophilic IL in the mixture, it form a homogeneous liquid state. Despite of the incompatibility between a phosphonium cation with long alkyl chains and an imidazolium cation, the mixtures were obtained as homogeneous liquids owing to the compatibility of sulfonate anion of the zwitterion and the hydrophilic amino acid IL. These results suggested that the miscibility of hydrophilic and hydrophobic ILs are improved using zwitterionization of a hydrophobic IL.

In chapter 3, a series of mixtures containing phosphonium-type ILs with a hydrophilic moiety and hydrophilic ILs was prepared to construct nano-segregated IL systems. The author envisioned these systems as forming *nano-biphasic systems* where two incompatible IL nano-domains coexist homogeneously in the macroscopic scale. To construct nano-segregated structure consisting of a hydrophilic IL and a hydrophobic IL, the author focused on the phosphonium-type zwitterions having a hydrophilic anion. They prefer to form homogeneous complexes with lithium bis(trifluoromethanesulfonyl) imide ($LiTf_2N$) forming two adjacent ion pairs: a hydrophobic ion pair and a hydrophilic ion pair. The phase behavior of these hydrophobic IL/hydrophilic IL mixtures depended on their ionic structures, and some mixtures showed liquid crystalline behavior due to the

nano-segregation of their hydrophilic and hydrophobic parts. For example, a phosphonium-type IL with a sulfonate anion mixed with an ammonium-type IL containing multiple hydroxyl groups showed two liquid crystalline phases depending on the composition of the two components. As the increase of the mole fraction of the hydrophilic IL in the mixture, it form a columnar structure excluding the cubic structure. These results indicate that the obtained nano-segregated structures consist of hydrophilic inner domains surrounded by hydrophobic outer domains.

In chapter 4, the properties, such as polarity and viscosity, of the nano-domains in the nano-segregated IL systems obtained in chapter 3 were evaluated using dyes that selectively dissolved in either the hydrophilic or hydrophobic ILs. The author considered proving that two independent IL nano-domains with different properties exist in the system as the best way to verify the nano-biphasic IL systems. First, the author has selected suitable dyes that dissolved selectively in either the hydrophilic or hydrophobic ILs. Through investigating various dyes, the author discovered that 3,4'-dihexyl-2,2'-bithiophene and naphthol yellow S are suitable dyes that possesses both of the desired properties: selective dissolution and good solvatochromism. By comparing the UV-vis absorption spectra for these dyes in the nano-segregated system to those in the corresponding ILs, the author determined that the nano-segregated IL system contains two domains with differing polarities. The polarity of each IL domain was nearly the same as for the corresponding ILs. These results suggest that a nano-segregated mixture formed, which was termed a *nano-biphasic system*. In addition, the local viscosity of the nano-segregated system was evaluated by using fluorescent anisotropy measurement of dyes dissolved selectively in each IL nano-domain.

Chapter 5 presented the conclusions of this thesis and discussed of the potential future for work.

Though out this thesis, the author concluded that using zwitterions is a promising approach for combining two immiscible ILs in macroscopic scale. In addition, a combination of a phosphonium-type zwitterion/Li salt complex and a hydrophilic IL provides a nano-biphasic IL system. The author believe that the nano-biphasic systems are especially promising candidates for novel separations and reactions because of the large interfaces between the two incompatible IL nano-domains.

# List of publications

## Original papers

(1)”Gelation of an amino acid ionic liquid by the addition of a phosphonium-type zwitterion”

S. Taguchi, T. Matsumoto, T. Ichikawa, T. Kato and H. Ohno

*Chem. Commun*., 2011, **47**, 11342-11344.

[Chapter 2]

(2)”Nano-biphasic ionic liquid systems composed of hydrophobic phosphonium salts and a hydrophilic ammonium salt”

S. Taguchi, T. Ichikawa, T. Kato and H. Ohno

*Chem. Commun*., 2012, **48**, 5271-5273.

[Chapter 3]

(3)”Design and evaluation of nano-biphasic ionic liquid systems having highly polar and low polar domains”

S. Taguchi, T Ichikawa, T. Kato and H. Ohno

*RSC Adv*,. 2013, **3**, 23222-23227

[Chapter 4]

## References

(1)”Hydrophobic and low-density amino acid ionic liquids”

J. Kagimoto, S. Taguchi, K. Fukumoto and H. Ohno

*J. Molecular Liq*., 2010, **153**, 133-138

(2)”Induction of thermotropic bicontinuous cubic phases in liquid-crystalline ammonium and phosphonium salts”

T. Ichikawa, M. Yoshio, A. Hamasaki, S. Taguchi, F. Liu, X. Zeng, G. Ungar, H. Ohno and T. Kato

*J. Am. Chem. Soc*., 2012, **134**, 2634-2643

(3)”Co-organisation of ionic liquids with amphiphilic diethanolamines: construction of 3D continuous ionic nanochannels through the induction of liquid-crystalline bicontinuous cubic phases”

T. Ichikawa, M. Yoshio, S. Taguchi, J. Kagimoto, H. Ohno and T. Kato

*Chem. Sci*., 2012, **3**, 2001-2008

(4)”3D anhydrous proton-transporting nanochannels formed by self-assembly of liquid crystals composed of a sulfobetaine and a sulfonic acid”
B. Soberats, M. Yoshio, T. Ichikawa, S. Taguchi, H. Ohno and T. Kato
*J. Am. Chem. Soc.*, 2013, **135**, 15286–15289

(5)”Poly-ionic liquids as new hydrogel materials: synthesis, characterization and application”
J. Bandomir, A. Schulz, S. Taguchi, S. Petersen, U. Kragl, H. Ohno and K. Sternberg
*Biomed Tech*., in press.